

Phosphate Ester Hydrolysis by Hydroxo Complexes of Trivalent Lanthanides Stabilized by 4-Imidazolecarboxylate

Francisco Aguilar-Pérez, Paola Gómez-Tagle, Elisa Collado-Fregoso, and Anatoly K. Yatsimirsky*

Facultad de Química, Universidad Nacional Autónoma de México, 04510 México D.F., México

Received June 8, 2006

The anion of 4-imidazolecarboxylic acid (HL) stabilizes hydroxo complexes of trivalent lanthanides of the type $ML(OH)^+$ ($M = La, Pr$) and $M_2L_n(OH)_{6-n}$ ($M = La, n = 2, 3; M = Pr, n = 2, 3; M = Nd, Eu, Dy, n = 1-3$). Compositions and stability constants of the complexes have been determined by potentiometric titrations. Spectrophotometric and 1H NMR titrations with Nd(III) support the reaction model for the formation of hydroxo complexes proposed on the basis of potentiometric results. Kinetics of the hydrolysis of two phosphate diesters, bis(4-nitrophenyl) phosphate (BNPP) and 2-hydroxypropyl 4-nitrophenyl phosphate (HPNPP), and a triester, 4-nitrophenyl diphenyl phosphate (NPDPP), in the presence of hydroxo complexes of five lanthanides were studied as a function of pH and metal and ligand concentrations. With all lanthanides and all substrates, complexes with the smallest n , that is $M_2L_2(OH)_4$ for La and Pr and $M_2L(OH)_5$ for Nd, Eu, and Dy, exhibited the highest catalytic activity. Strong inhibitory effects by simple anions (Cl^- , NO_3^- , $(EtO)_2PO_2^-$, AcO^-) were observed indicating high affinity of neutral hydroxo complexes toward anionic species. The catalytic activity decreased in the order $La > Pr > Nd > Eu > Dy$ for both diester substrates and was practically independent of the nature of cation for a triester substrate. The efficiency of catalysis, expressed as the ratio of the second-order rate constant for the ester cleavage by the hydroxo complex to the second-order rate constant for the alkaline hydrolysis of the respective substrate, varied from ca. 1 for NPDPP to 10^2 for HPNPP and to 10^5 for BNPP. The proposed mechanism of catalytic hydrolysis involves reversible bridging complexation of a phosphodiester to the binuclear active species followed by attack on the phosphoryl group by bridging hydroxide (BNPP) or by the alkoxide group of the deprotonated substrate (HPNPP).

Introduction

There is much current interest in the development of more efficient catalysts for the hydrolysis of phosphate esters of different types.¹ Hydroxo complexes of trivalent lanthanides constitute an important group of such catalysts.² Their development depends critically on the use of appropriate stabilizing ligands, which must prevent precipitation of metal hydroxide and at the same time allow for the formation of

active hydroxo complexes. This problem is common for catalysts based on hydroxo complexes of any metal but is especially difficult with lanthanides. Transition metal ions form stable complexes with neutral polyamine ligands, which do not reduce the total positive charge of the ion and therefore do not affect its electrophilicity but do prevent the hydroxide precipitation. Moreover, the electrophilicity of e.g. Zn(II) complexes with azomacrocycles is even higher than that of the aquo ion.³ Trivalent lanthanides do not form stable complexes with such ligands and require the presence of O-donors, preferably anionic groups for an efficient binding.⁴ Donor groups of this type are harmful for the catalytic

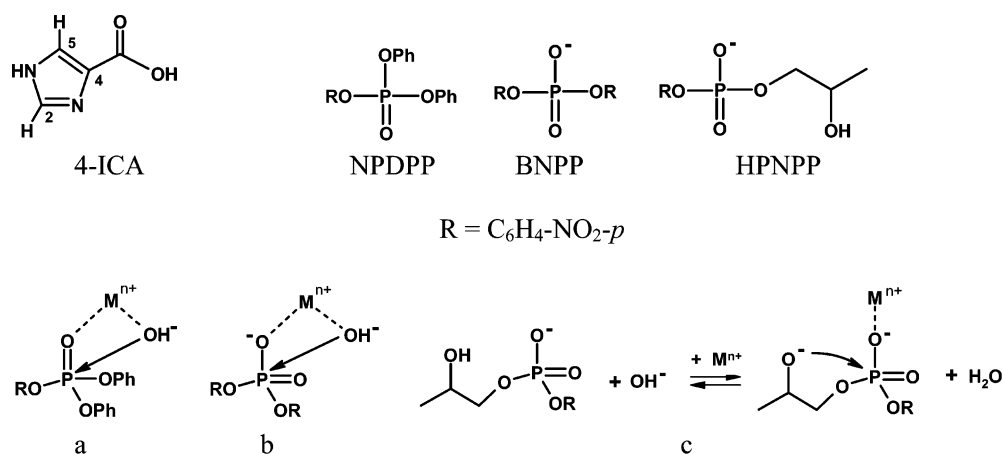
* To whom correspondence should be addressed. E-mail: anatoli@servidor.unam.mx. Fax: 55 5616 2010. Tel: 55 5622 3813.

(1) Recent reviews: (a) Yatsimirsky, A. K. *Coord. Chem. Rev.* **2005**, *249*, 1997. (b) Morrow, J. R.; Iranzo, O. *Curr. Opin. Chem. Biol.* **2004**, *8*, 192. (c) Morales-Rojas, H.; Moss, R. A. *Chem. Rev.* **2002**, *102*, 2497. (d) Liu, C. L.; Wang, M.; Zhang, T. L.; Sun, H. Z. *Coord. Chem. Rev.* **2004**, *248*, 147. (e) Brown, R. S.; Neverov, A. A. *J. Chem. Soc., Perkin Trans. 2* **2002**, 1039. (f) Williams, N. H. *Biochim. Biophys. Acta* **2004**, *279*, 1697. (g) Molenveld, P.; Engbersen, J. F. J.; Reinhoudt, D. N. *Chem. Soc. Rev.* **2000**, *75*, 29. (h) Kramer, R. *Coord. Chem. Rev.* **1999**, *182*, 243. (i) Williams, N. H.; Takasaki, B.; Wall, M.; Chin, J. *Acc. Chem. Res.* **1999**, *32*, 485.

(2) Reviews on lanthanide catalysis: (a) Lim, S.; Franklin, S. J. *Cell. Mol. Life Sci.* **2004**, *61*, 2184. (b) Schneider, H.-J.; Yatsimirsky, A. K. In *Metal Ions in Biological Systems*; Sigel, A., Sigel, H., Eds.; M. Dekker, Inc.: New York and Basel, 2003; Vol. 40, p 369. (c) Franklin, S. J. *Curr. Opin. Chem. Biol.* **2001**, *5*, 201. (d) Komiyama, M.; Takeda, N.; Shigekawa, H. *Chem. Commun.* **1999**, 1443. (e) Blasko, A.; Bruce, T. C. *Acc. Chem. Res.* **1999**, *32*, 475.

(3) Kimura, E.; Koike, T. *Adv. Inorg. Chem.* **1997**, *44*, 229.

Scheme 1



activity. Already in the first systematic studies of lanthanide catalysis in phosphodiester hydrolysis, additions of anionic ligands were found to produce inhibitory effects.⁵ However, it was demonstrated later that the attachment of carboxyl groups to an azamacrocyclic ligand increased the phosphodiesterolytic activity of Eu(III) complexes, although the type of active species was not identified.⁶ Recent more detailed studies with lanthanide complexes of macrocyclic ligands with attached carboxyl groups show that a high activity may be achieved by rising pH above 10.⁷ Apparently, a strongly basic medium is required to induce the formation of active hydroxo complexes even in the presence of an anionic ligand, but the type of reactive species again remained unidentified and only lower, poorly active hydroxo complexes predominating in pH range 8–9 were detected.

Recently we reported a very high phosphodiesterolytic activity of La(III) hydroxo complexes stabilized by anions of simple α -amino acids such as glycine or *N,N*-dimethylglycine at pH about 9 attributed to neutral binuclear species of the composition La₂L₂(OH)₄.⁸ These as well as the aforementioned results indicate that lanthanide complexes of anionic carboxylate ligands may still possess high catalytic activity provided the ligand structure allows formation of hydroxo complexes at reasonably low pH values.⁹ However, the reported⁸ system suffered from low stability which made virtually impossible a more detailed study. The problem is that due to the high p*K*_a values of zwitterions, e.g. 9.6 for glycine, such ligands remain largely protonated in the pH range 8–9 where catalytically active hydroxo species are formed and therefore cannot efficiently bind the metal ion.

To overcome this problem we tested several less basic structurally similar ligands and obtained satisfactory results with 4- and 2-imidazolecarboxylic acids (ICA). This paper reports the speciation and kinetics of catalytic hydrolysis of phosphate esters of different types with ICA complexes of five lanthanide cations.

It is worth to mention that recently a multitude of structurally characterized in solid state polynuclear lanthanide hydroxo complexes stabilized by simple ligands (often a natural α -amino acid) have been prepared via the so-called ligand-controlled hydrolysis procedure.^{10,11} At least partial motivation for these studies was the design of potentially active artificial phosphoesterases,¹⁰ but no catalytic activity with these complexes has been reported so far. On the other hand, for many catalytically active lanthanide systems the composition of solution hydroxo species remained unidentified due to well-known experimental difficulties of slow equilibration and easy precipitation of metal hydroxides. Using ICA as a stabilizing ligand allowed us to perform potentiometric titrations in a wide range of pH values at metal concentrations similar to those employed in kinetic experiments and to obtain more detailed and reliable speciation results than it was possible previously with other simple nonmacrocyclic ligands.

Although trivalent lanthanides were reported to be efficient catalysts for the hydrolysis of phosphate esters of different types,² the substrate specificity of lanthanide catalysis with a given active species has not yet been investigated and this is one of the aspects of this study. Model substrates typically employed for kinetic studies and used in this paper are two diesters, bis(4-nitrophenyl) phosphate (BNPP, a model for DNA hydrolysis) and 2-hydroxypropyl 4-nitrophenyl phosphate (HPNPP, a model for RNA hydrolysis), and a triester, 4-nitrophenyl diphenyl phosphate (NPDPP, a model for hydrolysis of toxic phosphates). Scheme 1 shows their chemical structures and illustrates generally accepted mech-

(4) Choppin, G. R. In *Lanthanide Probes in Life, Chemical and Earth Sciences*; Bünzli, J.-C. G., Choppin, G. R., Eds.; Elsevier: Amsterdam, 1989; p 1.

(5) Schneider, H.-J.; Rammo, J.; Hettich, R. *Angew. Chem., Int. Ed. Engl.* **1993**, *32*, 1716.

(6) Roigk, A.; Yescheulova, O. V.; Fedorov, Y. V.; Fedorova, O. A.; Gromov, S. P.; Schneider, H.-J. *Org. Lett.* **1999**, *1*, 833.

(7) Chang, C. A.; Wu, B. H.; Kuan, B. Y. *Inorg. Chem.* **2005**, *44*, 6646.

(8) Medrano, F.; Calderón, A.; Yatsimirsky, A. K. *Chem. Commun.* **2003**, 1968.

(9) Other lanthanide–amino acid catalytic systems: (a) Torres, J.; Brusoni, M.; Peluffo, F.; Kremer, C.; Domínguez, S.; Mederos, A.; Kremer, E. *Inorg. Chim. Acta* **2005**, *358*, 3320. (b) Calderón, A.; Yatsimirsky, A. K. *Inorg. Chim. Acta* **2004**, *357*, 3483. (c) Kalesse, M.; Loos, A. *Bioorg. Med. Chem. Lett.* **1996**, *6*, 2063. (d) Branum, M. E.; Que, L., Jr. *J. Biol. Inorg. Chem.* **1999**, *4*, 593.

(10) (a) Zheng, Z. *Chem. Commun.* **2001**, 2421. (b) Wang, R.; Liu, H.; Carducci, M. D.; Jin, T.; Zheng, C.; Zheng, Z. *Inorg. Chem.* **2001**, *40*, 2743.

(11) (a) Xu, G.; Wang, Z.-M.; He, Z.; Lu, Z.; Liao, C.-S.; Yan, C.-H. *Inorg. Chem.* **2002**, *41*, 6802. (b) Mahé, N.; Guillou, O.; Daiguebonne, C.; Gérault, Y.; Caneschi, A.; Sangregorio, C.; Chane-Ching, J. Y.; Car, P. E.; Roisnel, T. *Inorg. Chem.* **2005**, *44*, 7743.

anisms of catalysis by metal hydroxo complexes. Mechanisms of hydrolysis of BNPP and NPDPP are similar and involve the nucleophilic attack of a presumably coordinated hydroxide anion on the metal-bound phosphoryl group (Scheme 1a,b), but the cleavage of HPNP proceeds as an intramolecular transesterification, Scheme 1c. The absence of general base catalysis even with a very strong piperidine base (pK_a 11.12) indicates a mechanism with an initial equilibrium deprotonation of the 2-hydroxy group.¹² Such a mechanism operates also in catalytic hydrolysis of HPNPP by Zn(II) hydroxo complexes.^{13,14} Apparently the mechanistic differences mentioned above may lead to certain substrate specificity of lanthanide catalysis with esters of different types.

Experimental Section

Materials. Bis(4-nitrophenyl) phosphate (Aldrich) was recrystallized from ethanol–water. 2-Hydroxypropyl 4-nitrophenyl phosphate and 4-nitrophenyl diphenyl phosphate were prepared according to literature procedures.^{12,15} Diethyl phosphate was synthesized by controlled hydrolysis of triethyl phosphate and isolated as the barium salt, $Ba((EtO)_2PO_2)_2$, as described in ref 16 and then recrystallized from ethanol–water. 4-Imidazolecarboxylic acid (Aldrich), Tris base [tris(hydroxymethyl)aminomethane, Sigma], sodium salts (NaCl, $NaNO_3$, and NaAcO, Aldrich), methylamine as 40 wt % aqueous solution, and reagent grade lanthanide(III) perchlorates as 40 wt % aqueous solutions all from Aldrich were used as supplied. The concentration of methylamine in standard solutions, 0.1–0.15 M, was determined by titration against standard HCl solutions. The concentration of metal ions in stock solutions was determined by titration with ethylenediaminetetraacetic acid with Xylenol Orange as indicator. Distilled and deionized water (Barnstead Nanopure system) was used.

Potentiometry. Potentiometric titrations were performed by following general recommendations.¹⁷ All titrations were performed in a 50-mL thermostated cell kept under nitrogen at 25 ± 0.1 °C. The initial volume of titrating solution was 25 mL. The ionic strength was kept constant with 0.05 M NaCl. Measurements of pH were carried out using an Orion model 710-A research digital pH meter while the titrant solution was added to the system in small increments. The details of electrode calibration were described previously.¹⁸ The experimental determined pK_a values for $MeNH_3^+$ and 4-ICA were 10.67 ± 0.03 (literature value 10.64 at 25 °C and zero ionic strength¹⁹) and 6.23 ± 0.03 (reported $pK_a = 6.08$ was determined in 23.3% ethanol at 30 °C).²⁰ Titrations of 4-ICA and its mixtures with lanthanide salts were performed in the concentration range 1–6 mM of each component; 0.2 equiv of NaOH/mol of 4-ICA was always added to stock solution to form the 4-ICA anion and enhance solubility. The program *HYPERQUAD 2003*, version 3.0.51,²¹ was used to calculate all equilibrium constants.

The overall formation constants of monohydroxo species of lanthanides and their respective dimers were taken from the literature:^{19,22} $\log \beta(LaOH) = -9.06$, $\log \beta(La_2OH_2) = -17.4$; $\log \beta(PrOH) = -8.80$, $\log \beta(Pr_2OH_2) = -15.5$; $\log \beta(NdOH) = -8.45$, $\log \beta(Nd_2OH_2) = -13.9$; $\log \beta(EuOH) = -8.3$; $\log \beta(DyOH) = -8.12$. Species distribution diagrams were calculated by using *HYSS 2000* software^{21b} (*Hyperquad Simulation and Speciation*) and *Species*, ver. 0.8 (Academic Software 1999), by D. L. Pettit. *HyperChem*, ver. 7.5, was used for molecular modeling (molecular mechanics AMBER and semiempirical PM3 calculations).

Kinetics. Kinetic measurements were performed on a Hewlett-Packard 8453 diode array spectrophotometer equipped with a thermostated cell compartment (recirculating water bath ± 0.1 °C). Reaction solutions were prepared by combining appropriate amounts of metal and ligand stock solutions to the desired volume, and pH was adjusted by adding small volumes of strong acid or base solutions as necessary. Reactions were initiated by adding an aliquot of the substrate solution.

The course of BNPP, HPNPP, and NPDPP cleavage was monitored spectrophotometrically by the appearance of 4-nitrophenolate anion at 400 nm. Stock solutions of BNPP and HPNPP were freshly prepared in water. Stock solutions of NPDPP were prepared in dry acetonitrile. Kinetic measurements used 40 μ M substrate and varying concentrations of metal salts and 4-ICA, in 10 mM TRIS·HCl buffer at 25 °C. The total chloride concentration was kept constant at 10 mM by adding the required amounts of NaCl. The observed first-order rate constants (k_{obs}) were calculated by the integral method from at least 90% conversion or from initial rates for slow reactions. The second-order rate constants for the cleavage of substrates by active hydroxo complexes were calculated by linear regression from the plots of k_{obs} vs species concentration. In all cases the correlation coefficients were better than 0.97.

NMR Spectroscopy. ¹H NMR spectra were recorded on a Varian Gemini 300 NMR spectrometer in D₂O.

Results and Discussion

Composition and Stability of Hydroxo Complexes.

Composition and formation constants for hydroxo complexes of lanthanide with ICA as the stabilizing ligand were determined by potentiometric titrations. We observed improved system stability and better reproducibility of pH readings when methylamine was used instead of NaOH as a base probably because of the avoidance of local sharp boosts in hydroxide concentration. Methylamine does not form any detectable complexes with trivalent lanthanides in water and therefore does not affect the species distribution. For Nd(III) additional spectrophotometric and ¹H NMR titrations were performed. Results obtained with both isomers of ICA were very much similar. Therefore, in the following experiments only one isomer, i.e., 4-ICA, was employed.

Titrations of free ligand and its mixtures with lanthanides at pH below 7 (not shown), where formation of hydroxo complexes is negligible, allowed us to determine pK_a value of the ligand and stability constants of its binary complexes with lanthanides, summarized in Table 1. The basicity of

(12) Brown, D. M.; Usher, D. A. *J. Chem. Soc.* **1965**, 6558.

(13) Yang, M.-Y.; Iranzo, O.; Richard, J. P.; Morrow, J. R. *J. Am. Chem. Soc.* **2005**, *127*, 1064.

(14) Feng, G.; Mareque-Rivas, J. C.; Torres Martín de Rosales, R.; Williams, N. H. *J. Am. Chem. Soc.* **2005**, *127*, 13470.

(15) Gulick, W. M., Jr.; Geske, D. H. *J. Am. Chem. Soc.* **1966**, *88*, 2928.

(16) Kyogoku, Y.; Iitaka, Y. *Acta Crystallogr.* **1966**, *21*, 49.

(17) Martell, A. E.; Motekaitis, R. J. *Determination and Use of Stability Constants*, 2nd ed.; John Wiley & Sons: New York, 1992.

(18) Gómez-Tagle, P.; Yatsimirsky, A. K. *Inorg. Chem.* **2001**, *40*, 3786.

(19) Smith, R. M.; Martell, A. E. *Critical Stability Constants*; Plenum Press: New York, 1976; Vols. 2–4.

(20) Cowgill, R. W.; Clark, W. M. *J. Biol. Chem.* **1952**, *198*, 33.

(21) (a) Gans, P.; Sabatini, A.; Vacca, A. *Talanta* **1996**, *43*, 1739. (b) Alderlghi, L.; Gans, P.; Ienco, A.; Peters, D.; Sabatini, A.; Vacca, A. *Coord. Chem. Rev.* **1999**, *184*, 311.

(22) Rizkalla, E. N.; Choppin, G. R. In *Handbook on the Physics and Chemistry of Rare Earths*; Gschneider, K. A., Jr., Eyring, L., Eds.; Elsevier Science Publishers BV: Amsterdam, 1991; Vol. 15, p 393.

Table 1. Logarithms of the Overall Formation Constants of Lanthanide Complexes with 4-ICA at 25 °C and Ionic Strength 0.05 M^a

species	constant ^b	M = La(III)	M = Pr(III)	M = Nd(III)	M = Eu(III)	M = Dy(III)
LH	pK_a	6.23 ± 0.03				
ML	β_1	3.84 ± 0.09	4.20 ± 0.06	4.22 ± 0.05	4.4 ± 0.1	4.46 ± 0.02
ML ₂	β_2	7.1 ± 0.2	7.62 ± 0.06	7.72 ± 0.08	8.0 ± 0.2	8.08 ± 0.01
ML ₃	β_3		10.7	10.38 ± 0.02	10.5 ± 0.6	10.8
ML(OH)	β_{11-1}	-5.1 ± 0.3	-4.6 ± 0.4			
M ₂ L ₃ (OH) ₃	β_{23-3}		-11.0 ± 0.1	-9.8 ± 0.3	-7.9 ± 0.6	-7.5 ± 0.1
M ₂ L ₂ (OH) ₄	β_{22-4}	-25.7 ± 0.1	-22.4 ± 0.2	-21.8 ± 0.2	-19.1 ± 0.4	-19.3 ± 0.2
M ₂ L(OH) ₅	β_{21-5}			-33.4 ± 0.3	-31.5 ± 0.3	-31.8 ± 0.1

^a The constants are mean values from at least three titrations at different total metal and ligand concentrations; L is the monoanion of 4-ICA ^b Formation constants for hydroxo complexes β_{mh} are defined in accordance with eqs 1–4.

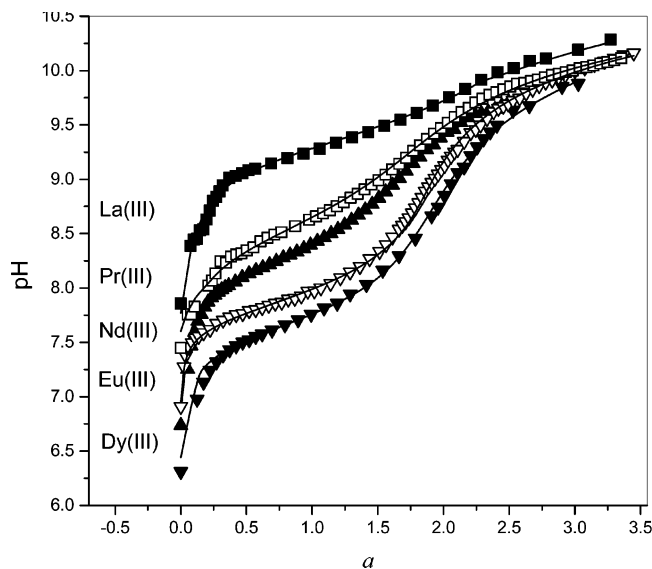


Figure 1. Titration curves for the mixtures of 3 mM 4-ICA and 2 mM lanthanide perchlorate with 0.13 M MeNH₂ as a base starting from the point of complete neutralization of 4-ICA. *a* is the number of moles of MeNH₂ added per 1 mol of the metal ion. Solid lines are the fitting curves generated by HYPERQUAD in accordance with equilibrium constants given in Table 1.

4-ICA is ca. 3 orders of magnitude lower than that of natural α -amino acids. Nevertheless this ligand forms even more stable complexes with trivalent lanthanides: for comparison $\log\beta_1 = 3.1, 3.26$ and 3.6 for complexes of La(III), Nd(III) and Dy(III) with glycine.²³ As a result the degree of complex formation with ICA in basic solutions becomes big enough to allow one to perform titration experiments up to high pH values without a significant excess of the ligand. The values of $\log\beta_1$ and $\log\beta_2$ increase as expected on going from La(III) to heavier, more acid cations. The values of $\log\beta_3$ are less accurate and do not show a clear tendency probably due to larger errors of determination.

Figure 1 shows a set of typical titration curves obtained for mixtures of lanthanides with 4-ICA taken at molar ratio M:L = 2:3 at pH above 7. Under these conditions the ligand is already completely deprotonated and the consumption of added base is due only to the formation of hydroxo species. A qualitative inspection of the curves shows that on going from La(III) to Dy(III) the stability of hydroxo complexes increases (the curves are progressively shifted to lower pH values) but even with Dy(III) there is no clear upward break

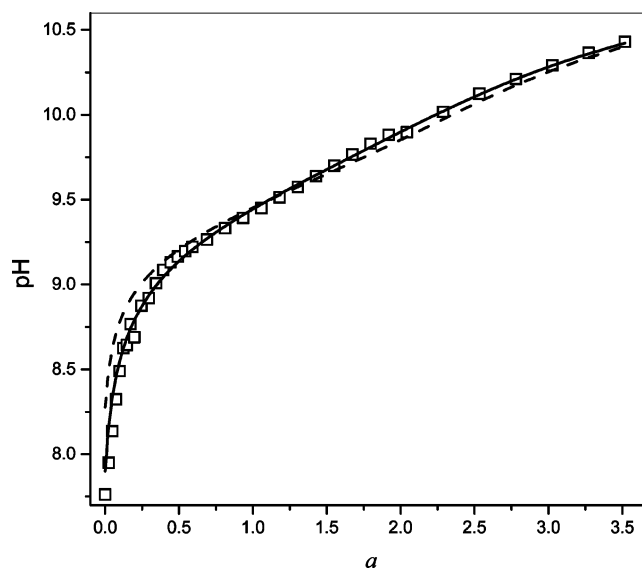


Figure 2. Titration curve for the mixture of 6 mM 4-ICA and 2 mM La(III) perchlorate. The dashed line shows the best fit for a model involving only one hydroxo complex ML(OH)₂, and the solid line shows the fitting for a model involving ML(OH)₂ and ML(OH)⁺ complexes.

in pH at the end of titration expected in a case of formation of a single hydroxo complex. Instead one observes a short plateau range followed by a faster increase in pH in a wide interval of *a* values (*a* is the molar ratio of total added base to total metal) from 1.5 to 2.5. Apparently there is a set of complexes of different stoichiometries formed consecutively on addition of base.

A preliminary analysis of the titration results was performed by examination of the pH-dependence of the Bjerrum function \bar{n} defined as the average number of hydroxo anions bound per mole of the metal ion detailed in Supporting Information. Figures 1S and 2S (Supporting Information) shows the respective plots for different metals and at different metal-to-ligand molar ratios. It follows from this analysis that for La(III) and Pr(III) the expected composition of hydroxo complexes $M_mL_l(OH)_h$ is such that *l*:*m* ratio is constant and low, probably unity, and the *h*:*m* ratio is 2 or lower, but for lanthanides of bigger atomic numbers the *l*:*m* ratio is variable decreasing on increasing the *h*:*m* ratio which has a limiting value of 2.5. Titration results for La(III) were fitted first to a simple model which involves just one hydroxo complex ML(OH)₂. An example of such fit is shown in Figure 2, dashed line. The theoretically calculated curve passes fairly close to the experimental points, but shows a significant deviation to higher pH values at low *a* values.

(23) Smith, R. M.; Martell, A. E. *Critical Stability Constants*; Plenum Press: New York, 1989; Vol. 6, p 1.

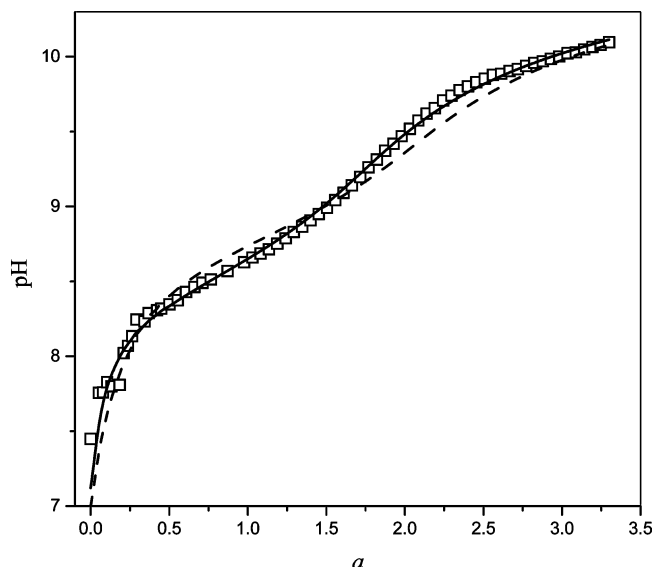


Figure 3. Titration curve for the mixture of 3 mM 4-ICA and 2 mM Pr(III) perchlorate. The dashed line shows the best fit for a model involving two hydroxo complexes $M_2L_2(OH)_4$ and $ML(OH)^+$, and the solid line shows the fitting for a model involving additional $M_2L_3(OH)_3$ complex.

This indicates the presence of another hydroxo complex with lower $h:m$ ratio. Indeed, inclusion of the monohydroxo species $ML(OH)$ in the reaction scheme greatly improves the fitting quality, Figure 2, solid line. Since hydroxide often serves as a bridging ligand we also tested the possible involvement of the respective binuclear complexes and found that the fitting quality to a model involving a combination of $ML(OH)$ and $M_2L_2(OH)_4$ species was somewhat better than to a model involving only mononuclear species (Table 1S in Supporting Information lists the sigma values for fittings to both models).

Fitting of the results for Pr(III) to the same model as for La(III) was not satisfactory. The dashed line in Figure 3

illustrates this situation. An increase in the slope of the titration curve at $a = 1.5$ suggests the presence of an additional complex of an intermediate composition $M:OH = 2:3$. Indeed inclusion of $M_2L_3(OH)_3$ complex in the reaction model allowed us to obtain a perfect fit of the titration results (Figure 3, solid line). Besides of $M_2L_3(OH)_3$ a set of complexes of composition $M_2L_l(OH)_3$ with $l = 2-4$ was tested and the complex with $l = 3$ was chosen on basis of a better statistics.

Titration results for Nd(III), Eu(III) and Dy(III) were significantly different from those for La(III) and Pr(III). The following procedure was applied to find the best reaction model. First the composition of the highest hydroxo complex was established from titration results at the lowest possible ligand concentration. For all three metals under such conditions we observed the predominant formation of a single hydroxo complex $M_2L(OH)_5$. Then in titrations with increasing ligand concentrations additional binuclear complexes were included with smaller number of hydroxo ligands and larger number of 4-ICA ligands. In all cases the best fit was obtained after the inclusion of only two additional complexes of compositions $M_2L_2(OH)_4$ and $M_2L_3(OH)_3$ which were observed also for Pr(III).

Figure 4 illustrates the procedure with results for Eu(III) as an example. The titration curve for 2 mM 4-ICA in the presence of 3 mM Eu(III), Figure 4A, can be satisfactorily fitted to just one equilibrium of formation of a single hydroxo complex $M_2L(OH)_5$. The shape of the titration curve under these conditions is very sensitive to the stoichiometry of the complex. Dash line and short dash line show the best fitting curves for models assuming complex stoichiometries altered by just one 4-ICA ligand ($M_2L_2(OH)_5$) or one hydroxide ($M_2L(OH)_4$), respectively. Figure 4B shows the titration curve for a mixture of 2 mM Eu(III) and 3 mM 4-ICA, that

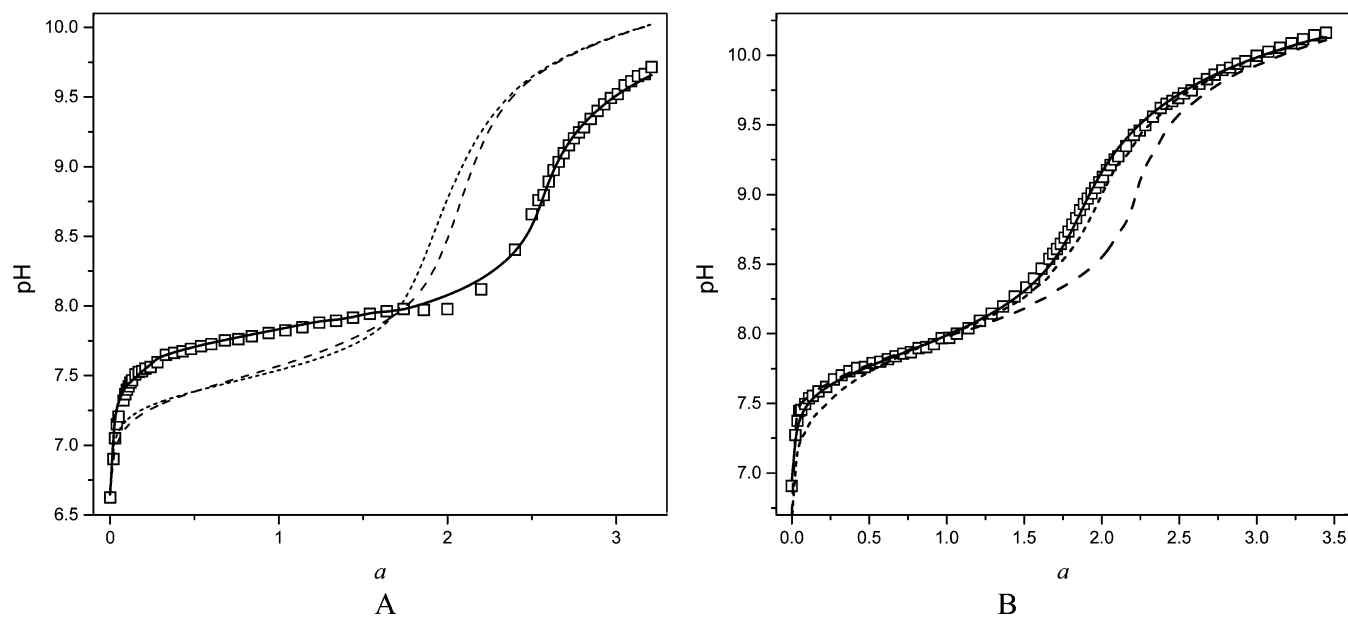


Figure 4. (A) Titration curve for the mixture of 2 mM 4-ICA and 3 mM Eu(III) perchlorate. The solid line shows the fitting for a model involving only the $M_2L(OH)_5$ complex, the dashed line shows the fitting for a model involving only $M_2L_2(OH)_5$ complex, and the short dashed line shows the fitting for a model involving only the $M_2L(OH)_4$ complex. (B) Titration curve for the mixture of 3 mM 4-ICA and 2 mM Eu(III) perchlorate. The dashed line shows the best fit for a model involving only the $M_2L(OH)_5$ complex, the short dashed line shows the fitting for $M_2L(OH)_5$ and $ML(OH)_2$ complexes, and the solid line shows the fitting for a model involving $M_2L(OH)_5$ and $M_2L_2(OH)_4$ complexes.

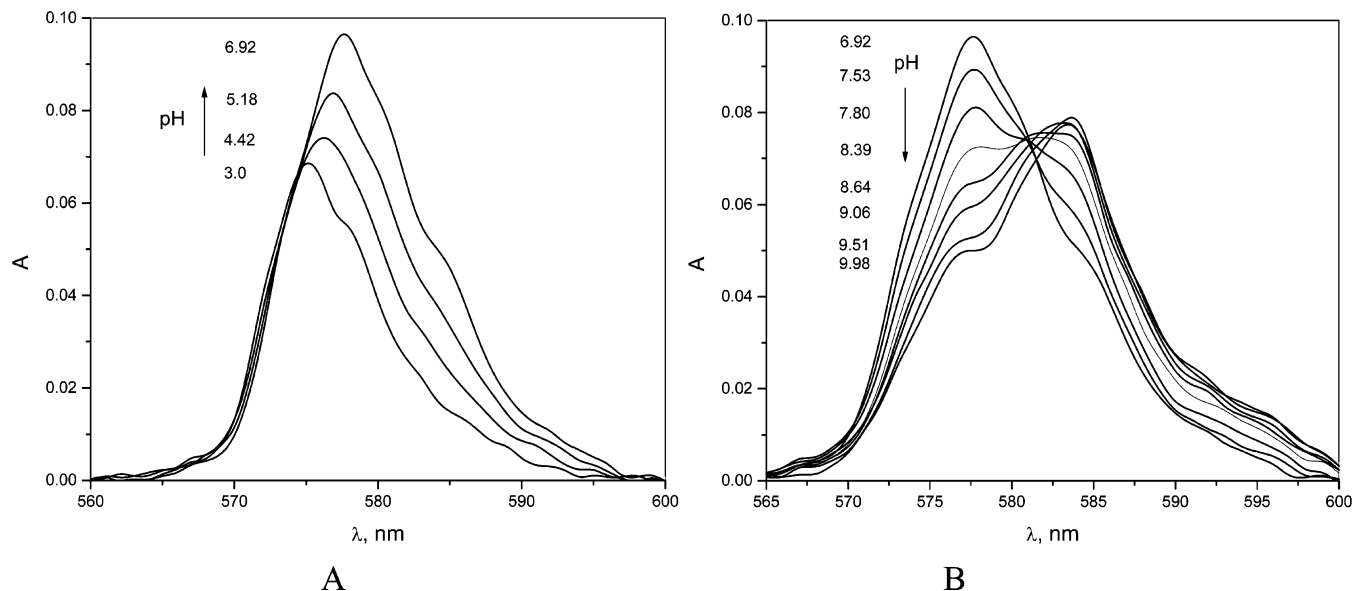
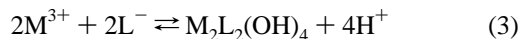
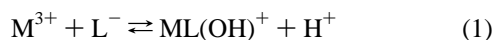


Figure 5. Absorption spectra of a mixture of 2 mM Nd(III) perchlorate and 2 mM 4-ICA in the hypersensitive region at increased pH values. The cuvette path length is 5 cm.

is under conditions of an excess of the ligand. The dash line is the best fitting curve for a model with a single $M_2L(OH)_5$ complex and it clearly passes below the experimental curve indicating the consumption of a smaller amount of hydroxide. The short dash line shows the fitting results for a model involving also a dihydroxo complex $ML(OH)_2$. The simulated fitting curve passes much closer to the experimental points, but is steeper at lower pH than the experimental curve. This reflexes a more rapid consumption of hydroxide, usually related to the formation of polynuclear complexes. Indeed, the model which involves a dimeric binuclear species $M_2L_2(OH)_4$ together with the previously established $M_2L(OH)_5$ complex allows one to obtain a nearly perfect fit shown by the solid line in Figure 4B. Fitting to the model which also involves the trihydroxo complex $M_2L_3(OH)_3$ observed for Pr(III), does not look visually different and therefore is not shown in Figure 4B, but statistical parameters of the fitting, especially at higher ligand concentrations were significantly better for such an extended model.

In conclusion, the analysis of potentiometric titration results at pH above 7 indicates the following set of equilibria:



Here L^- is the monoanion of 4-ICA. The fitting results for all titrations together with the respective statistical parameters are given in Supporting Information Table 1S. The average values of the formation constants which correspond to equilibria (1)–(4) are given in Table 1. Stability of all hydroxo complexes increases as expected on passing from La(III) to Dy(III). Additional information on the nature of

lanthanide complexes of 4-ICA was obtained from UV–vis and NMR titrations of Nd(III) system.

We chose Nd(III) for spectroscopic studies because this cation possesses a so-called hypersensitive absorption band in the range 570–595 nm, which undergoes relatively strong changes on coordination with different donor atoms.^{24–26} The substitution of coordinated water molecules by different donor atoms leads to an increase in the oscillator strength (f) calculated by integration of the absorption band.^{24,25,27} The carboxylate group produces the smallest effect, and groups with nitrogen donor atoms produce the largest increase in f . Hydroxide ion has an intermediate effect. Although the additivity of effects from several groups was not specially tested, it has been proposed that f value should be proportional to the number of donor atoms of ligands substituting water in the coordination sphere of the cation.^{24,27}

Figure 5 shows the absorption spectra of Nd(III) in the presence of an excess of 4-ICA within the hypersensitive range as a function of pH. The spectrum at pH 3 practically coincides with the spectrum of Nd(III) aquo ion. Raising the pH value from 3 to 7 is accompanied by an increase in absorbance and a small red shift of the maximum, Figure 5A. Further increase in pH above 7 produces a decrease in absorbance and further more significant red shift of the maximum, Figure 5B.

Assuming that the principal effect is due to the presence of bound heterocyclic ligand nitrogen donor atoms and hydroxide ions, we analyzed the results in terms of a possible correlation between the relative oscillator strength (f/f_0 , where

(24) Henrie, D. E.; Fellows, R. L.; Choppin, R. G. *Coord. Chem. Rev.* **1976**, *18*, 199.

(25) (a) Stephens, E. M.; Schoene, K.; Richardson, F. S. *Inorg. Chem.* **1984**, *23*, 1641. (b) Stephens, E. M.; Davis, S.; Reid, M. F.; Richardson, F. S. *Inorg. Chem.* **1984**, *23*, 4607.

(26) (a) Hancock, R. D.; Jackson, G.; Evers, A. *J. Chem. Soc., Dalton Trans.* **1979**, 1384. (b) Birnbaum, E. R.; Darnall, D. W. *Bioinorg. Chem.* **1973**, *3*, 15.

(27) Yang, W.; Gao, J.; Kang, J.; Yang, W. *J. Solution Chem.* **1997**, *26*, 105.

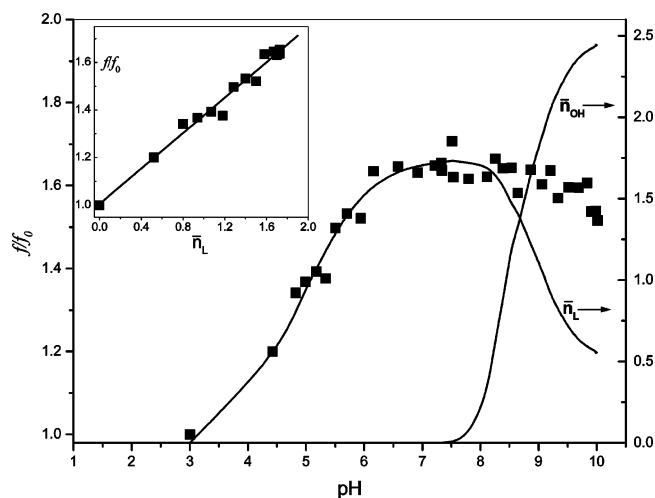


Figure 6. Relative oscillator strength (ff_0) of the hypersensitive band as a function of pH superimposed with the average number of bound 4-ICA (\bar{n}_L) and hydroxide (\bar{n}_{OH}) anions. Inset: Correlation between ff_0 and \bar{n}_L at pH below 7.3.

f_0 is the oscillator strength for aquo ion) and the average number of 4-ICA anions (\bar{n}_L) and hydroxide ions (\bar{n}_{OH}) bound to Nd(III). Figure 6 shows the plot of ff_0 vs pH superimposed with curves for \bar{n}_L and \bar{n}_{OH} . There is a good linear correlation between ff_0 and \bar{n}_L at pH below 7.3 where the fraction of hydroxo complexes is negligible, as shown in the inset in Figure 6. From the slope of the line in the inset, one can estimate that each nitrogen atom enhances the ff_0 by 37%. The relative oscillator strength for the Nd(DPA) $_3^{3-}$ complex (DPA is the dianion of dipicolinic acid) is 2.1,²⁵ which corresponds to the same increment by 37% for each nitrogen atom. Further spectral changes shown in Figure 5B reflect the formation of hydroxo complexes. A gradual decrease in absorption agrees with the expulsion of 4-ICA anions from the coordination sphere of the metal by hydroxide ligands, as was concluded from potentiometric titrations. In most basic solutions the oscillator strength decreases by approximately 10% as compared to its value at pH 7, the average number of bound 4-ICA anions decreases from 1.7 to 0.5, and the average number of bound OH $^-$ increases from 0 to 2.4. This means that the effect of hydroxide is approximately half of the effect of 4-ICA. A similar conclusion follows also from the comparison of spectra of Nd(III) complexes with DPA or malate recorded at high pH.²⁵

The absorption spectra of Nd(III) recorded in the presence of an excess of the metal salt over 4-ICA (Figure 3SA, Supporting Information) pass through an isosbestic point at 579 nm in accordance with expected formation of a single hydroxo complex under these conditions. The plot of the absorbance at a given wavelength vs pH perfectly follows the calculated species distribution diagram (Figure 3SB, Supporting Information).

The 1H NMR spectra of amino acids bound to Nd(III) have been extensively studied.²⁸ The analysis of complexation-induced shifts of the signals was usually performed on the basis of a theoretically derived equation which predicts that the magnitude and direction of the shift follow a $(3 \cos^2 \theta - 1)/r^3$ dependence, where r is the distance of the given proton from the metal ion and θ is the angle between

the distance vector and the principal molecular axis of the complex.²⁸ Although this assumption is valid only for axially symmetric systems, it was argued that under conditions of fast exchange between free and metal bound ligand, which is fulfilled for simple amino acid ligands and lanthanide cations, the averaging of the signal and the ligand position allows one to consider the system as pseudosymmetrical and the above equation still applies.^{28d}

Figure 7 shows the results of pH titration of free 4-ICA (solid squares) and the mixture of 2 mM 4-ICA with 2 mM Nd(III) (open squares) in D $_2$ O. The NMR spectrum of 4-ICA consists of two singlets in the range 7–8 ppm. Both signals undergo a downfield shift on protonation of the N-3 nitrogen, the magnitude of the shift being larger for the C-2 proton. Fitting of the results for the free ligand (solid lines in Figure 10) to the eq 5 for the protonation equilibrium (δ_L and δ_{LH} are the chemical shifts of anion and zwitterion of 4-ICA respectively) gives $pK_a = 6.3 \pm 0.2$ in good agreement with potentiometric titrations results in water.

$$\delta = (\delta_L + \delta_{LH}(10^{-pD}/K_a))/(1 + 10^{-pD}/K_a) \quad (5)$$

In the presence of Nd(III) in acid media both signals undergo downfield shifts with respect to their positions in the spectrum of protonated (zwitterionic) 4-ICA. On increasing pH the signal of C-2 proton moves further downfield, but the signal of C-5 proton moves in the opposite direction. At pH 7 the fraction of the anion of 4-ICA bound to Nd(III) reaches the maximum (90% from which 50% in NdL $^{2+}$ and 40% in NdL $_2^+$ species), but there are still less than 0.01% of mixed hydroxide complexes. Under these conditions the signal of C-2 proton appears shifted by 2.4 ppm downfield and the signal of C-5 proton shifted by ca. 0.1 ppm upfield from their positions in the 4-ICA anion. A similar titration experiment with 2 mM 4-ICA in the presence of 2 mM La(III) showed only a small downfield shift for both protons by ca. 0.1 ppm versus their positions in the free anion apparently due to the inductive effect of the metal cation. The inversion of the shift for C-5 proton indicates that at low pH some species should exist having a structure different from that at pH 7. We propose that at low pH a weak complex of Nd(III) with the zwitterionic form of 4-ICA (Chart 1) may contribute to the observed signal shift. In accordance with the $(3 \cos^2 \theta - 1)/r^3$ dependence, the direction of the complexation-induced shift is a function of the θ angle: the positive shift is observed if the angle is smaller than 55°, and the negative shift, for angles between 55 and 90°. A molecular model of this complex was generated, and assuming the position of the principal axis as indicated by the dash line, we found that the θ angles are equal 23.9 and 9.2° and distances from Nd(III) are 5.31 and 7.56 Å for protons at C-5 and C-2, respectively. Thus for this species both shifts should be positive and the shift for

(28) (a) Sherry, A. D.; Birnbaum, E. R.; Darnall, D. W. *J. Biol. Chem.* **1972**, *247*, 3489. (b) Sherry, Yoshida, C.; A. D.; Birnbaum, E. R.; Darnall, D. W. *J. Am. Chem. Soc.* **1973**, *95*, 3011. (c) Sherry, A. D. *J. Am. Chem. Soc.* **1977**, *99*, 5871. (d) Sherry, A. D.; Stark, C. A.; Ascenso, J. R.; Galdes, C. F. G. *J. Chem. Soc., Dalton Trans.* **1981**, 2078.

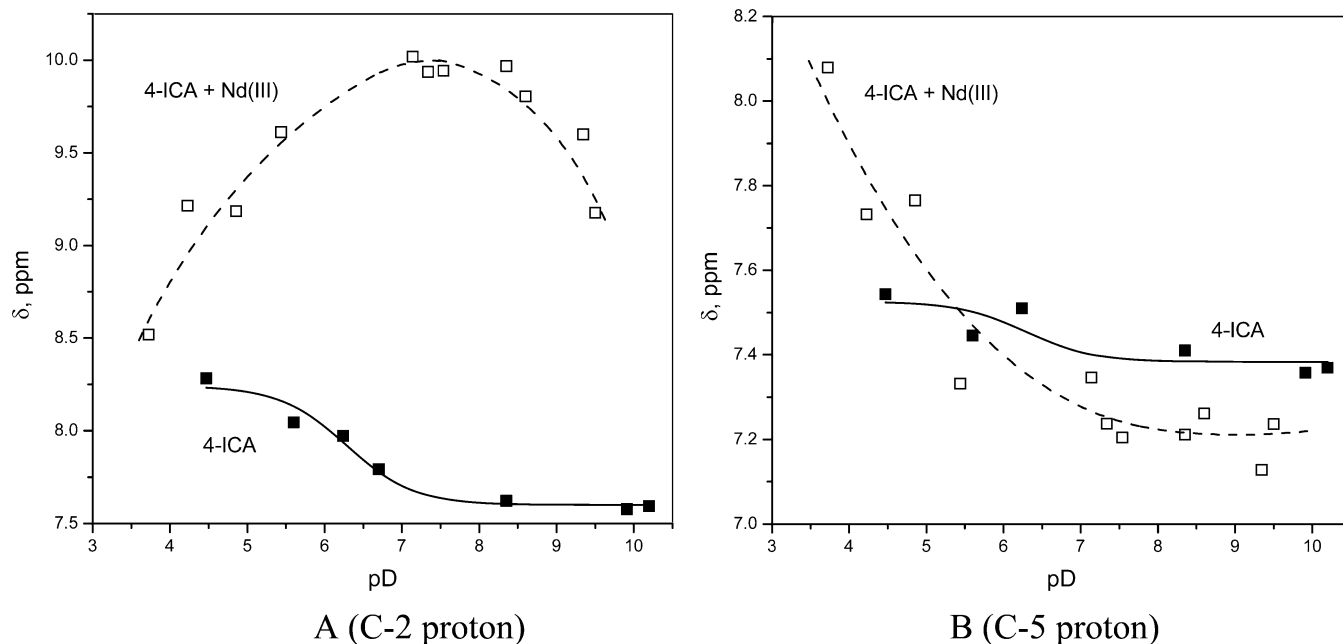
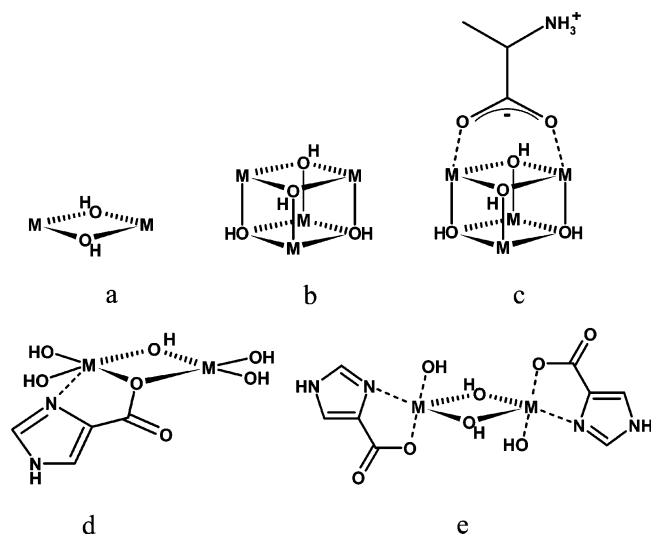


Figure 7. Chemical shifts of C-2 (A) and C-5 (B) protons of 4-ICA recorded at variable pD in a mixture of 2 mM 4-ICA and 2 mM Nd(III) (open squares) and for 4-ICA in the absence of added metal ion (solid squares). Dashed lines are drawn to visualize the tendency and are not the fitting curves. Solid lines are the theoretical fitting curves to eq 5.

Chart 1



C-5 proton should be larger than that for C-2. The position of the axis in the 1:1 complex with 4-ICA anion is very uncertain, but for the 1:2 complex one may consider the position of axis shown in Chart 1. The parameters obtained by using the respective model are $\theta = 79$ and 29° and $r = 5.49$ and 4.34 \AA for protons at C-5 and C-2, respectively. With these parameters the expected shift should be small and negative for the C-5 proton and large and positive for the C-2 proton, in accordance with results in Figure 7A,B.

In basic solutions above pH 7 complexes NdL^{2+} and NdL_2^+ are transformed into hydroxo complexes with a simultaneous increase in the concentration of the free 4-ICA. This should move the signal closer to the position observed for free ligand under conditions of a fast exchange between free and bound ligand. Indeed, such a trend more clearly seen for the C-2 proton is observed in Figure 7. Thus the NMR titration confirms the bidentate N,O-coordination of

4-ICA anion and agrees with the reaction scheme assuming a decreased M:L ratio in complexes with increased number of bound hydroxide ions.

Previously, we described the formation of a set of hydroxo complexes of general composition $\text{M}_2\text{L}_2(\text{OH})_n^{6-n}$, where L was Bis-Tris propane and n varied from 2 to 6 for the same series of lanthanide cations as those employed in this paper.¹⁸ With 4-ICA as a stabilizing ligand we find now a similar set of complexes of general composition $\text{M}_2\text{L}_n(\text{OH})_{6-n}$ with the only difference that the number of bound ligand molecules in this case is variable and decreases as the number of bound hydroxides increases. This difference is quite logical because Bis-Tris propane is a neutral ligand but 4-ICA is an anion, which indeed may compete with hydroxo anions for the coordination sphere of the metal ion. The fact that we observe formation of mononuclear hydroxo complexes only for La(III) and Pr(III) agrees with known higher tendency of heavier cations to aggregation.²⁹ Concerning the perhaps most unusual pentahydroxo complexes $\text{M}_2\text{L}(\text{OH})_5$ with just one stabilizing ligand/two metal ions, it is worth noting that we observed earlier the formation of $\text{M}_2\text{L}(\text{OH})_5^+$ species with $\text{M} = \text{Y(III)}$ and $\text{L} = \text{Bis-Tris propane}$.³⁰ Also the formation of binuclear pentahydroxo ligand-free catalytically active species $\text{La}_2(\text{OH})_5^+$ and $\text{La}_2(\text{OMe})_5^+$ in water³¹ and methanol,³² respectively, has been previously reported.

Possible structures of lanthanide hydroxo complexes stabilized by 4-ICA may be discussed on the basis of several reported crystal structures of both hydroxo and amino acid lanthanide complexes. The majority of structurally character-

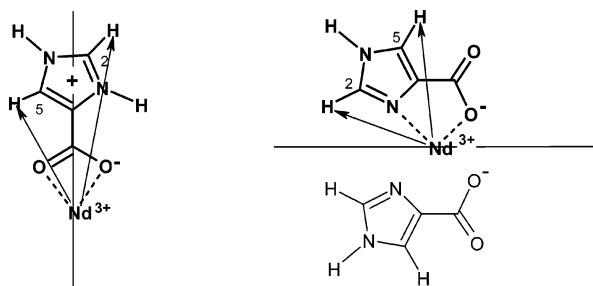
(29) Baes, C. F., Jr.; Mesmer, R. E. *The Hydrolysis of Cations*; Wiley: New York, 1976.

(30) Gómez-Tagle, P.; Yatsimirsky, A. K. *J. Chem. Soc., Dalton Trans.* **2001**, 2663.

(31) Hurst, P.; Takasaki, B. K.; Chin, J. *J. Am. Chem. Soc.* **1996**, *118*, 9982.

(32) Neverov, A. A.; Brown, R. S. *Inorg. Chem.* **2001**, *40*, 3588.

Scheme 2



ized lanthanide hydroxo complexes have a M:OH ratio 1:1. A structural motif often encountered in these compounds involves the planar four-membered ring with both hydroxides as bridging ligands shown in Scheme 2. Binuclear complexes of the composition $M_2(OH)_2^{4+}$ in water²⁹ as well as $M_2(MeO)_2^{4+}$ in methanol³² were reported on the basis of titration results for many lanthanides, and they probably possess similar structures. Another common structure involves tetranuclear complexes with a cuboidlike core $M_4(OH)_4^{8+}$, Scheme 2.¹⁰ However, as will be shown below, catalytically active forms are higher hydroxo complexes with M:OH ratios 1:2 or 1:2.5. There are several examples of complexes of this type structurally characterized in the solid state including $Eu_2(OH)_4(OOCC_6H_4COO)$,³³ $M_2(OH)_4(CO_3)$, and $M(OH)_2(NO_3)$.³⁴ All these compounds have polymeric or layered structures in which all hydroxide ligands are bridging the metal centers. In many cases, each pair of lanthanide cations is bridged by two hydroxide ions, but in the structure of $Eu_2(OH)_4(OOCC_6H_4COO)$ a triply bridged fragment $M(OH)_3M$ also exists.

Reported crystal structures of lanthanide complexes with amino acids mainly involve zwitterions as the ligands.³⁵ Interestingly, the amino group remains protonated even in some hydroxo complexes possessing a $M_4(OH)_4^{8+}$ core, Scheme 2.¹⁰ Of course, conservation of protonated amino group in the presence of coordinated hydroxide occurs because of high basicity of this group in natural amino acids. Chelate N,O coordination expected for much less basic 4-ICA was observed in complexes with *N,N*-bis(hydroxyethyl)glycine³⁶ or EDTA.^{10a} An unusual coordination mode was observed in the complex $Na_{10}[La_4(\mu_3-OH)_4(EDTA)_4](ClO_4)_2$ ^{10a} with one of carboxylate groups of EDTA acting as a bridge between two La(III) ions of a cuboid structure. This coordination mode could explain the ability of 4-ICA to serve as a sole stabilizing ligand for binuclear $M_2L(OH)_5$ species, as shown in Scheme 2. For the tetrahydroxo $M_2L_2(OH)_4$ complex a symmetrical structure shown in Scheme 2 seems to be the most appropriate.

Kinetics of the Catalytic Hydrolyses. Most of the kinetic studies in this work were performed using BNPP as the

substrate. As a first step the reactivity was studied as a function of pH at fixed metal and ligand concentrations to correlate the rate–pH profiles with species distribution diagrams and to identify the reactive species. Figure 8A–E show pH profiles of observed first-order rate constants (k_{obs}) for the hydrolysis of BNPP by 2 mM metal ion in the presence of 2 mM 4-ICA superimposed with the species distribution diagrams. Obviously the most reactive species for any metal is always the highest hydroxo complex. For La(III) and Pr(III) the reactivity can be attributed to $M_2L_2(OH)_4$ complexes and for Nd(III) and Eu(III) to $M_2L(OH)_5$ complexes, respectively. For Dy(III) there is also a noticeable contribution from lower hydroxo complexes.

The fact that the reactivity tracks the pH profile for a certain species means that the k_{obs} is proportional to the concentration of a given species. This is illustrated for Nd(III) in Figure 9, where k_{obs} values are plotted vs the calculated concentration of the $Nd_2L(OH)_5$ complex at each pH (solid squares).

The situation however is not as simple as it seems from these results. When a similar k_{obs} vs pH plot was obtained again for 2 mM Nd(III) but with 4 mM 4-ICA, it showed again a perfect correlation with the distribution curve for $Nd_2L(OH)_5$ complexes, but the values of k_{obs} at the given complex concentration were significantly lower (Figure 9, open squares). Similar results were obtained with all cations studied. We see therefore that the reaction kinetics is first-order in the highest hydroxo complex, but there is also an inhibitory effect of the excess of the ligand.

Further kinetic studies involved measurements of k_{obs} at fixed pH but at variable metal and ligand concentrations. All cations behaved similarly. The results for Nd(III) at pH 9 are shown in Figure 10 as an illustration. Two types of experiments were performed: simultaneous variation in metal and ligand concentrations taken at a constant molar ratio; variation in metal concentration in the presence of fixed concentration of the ligand taken in an excess. Figure 10A shows the results for both types of experiments. Solid triangles and open squares correspond to results obtained at fixed 4-ICA:Nd(III) molar ratios 1:1 and 1.5:1, respectively. Both dependences are roughly linear with some tendency to “saturation”. Solid squares correspond to results obtained at fixed 6 mM 4-ICA and variable Nd(III). This plot is obviously nonlinear. The solid line corresponds to a quadratic dependence.

These plots cannot be interpreted directly in terms of a reaction order because the concentration of active species is not a linear function of total metal and ligand concentrations. In Figure 10B all these results are replotted showing k_{obs} as a function of $[Nd_2L(OH)_5]$ calculated in each point in accordance with stability constants given in Table 1. The plots are linear now, but their slopes are smaller in reaction series obtained with higher 4-ICA concentrations. The slope for the 1:1 mixture (solid triangles) is very close to the slope of the plot in Figure 9 (solid squares) obtained also for the 1:1 mixture but at variable pH. The slope for results obtained with 6 mM 4-ICA is close to that of the plot in Figure 9 (open squares) obtained for the 2:1 metal-to-ligand mixture

(33) Serre, C.; Millange, F.; Marrot, J.; Férey, G. *Chem. Mater.* **2002**, *14*, 2409.

(34) Wickleder, M. S. *Chem. Rev.* **2002**, *102*, 2011.

(35) Kremer, C.; Torres, J.; Domínguez, S.; Mederos, A. *Coord. Chem. Rev.* **2005**, *249*, 567.

(36) (a) Inomata, Y.; Takei, T.; Howell, F. S. *Inorg. Chim. Acta* **2001**, *318*, 201. (b) Messimeri, A.; Raptopoulou, C. P.; Nastopoulos, V.; Terzis, A.; Perlepes, S. P.; Papadimitriou, C. *Inorg. Chim. Acta* **2002**, *336*, 8.

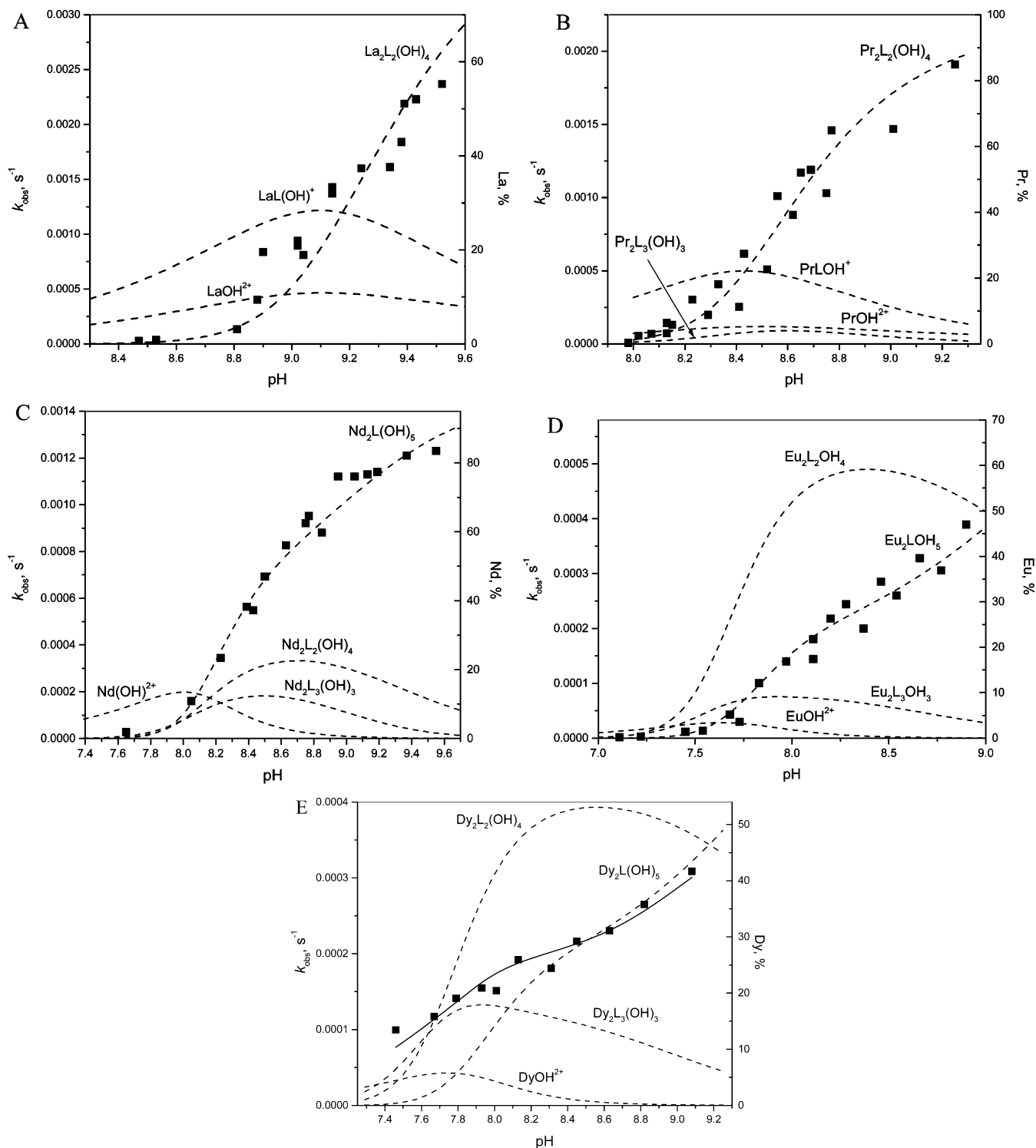


Figure 8. Observed first-order rate constants for the hydrolysis of BNPP by different metals in the presence of 2 mM lanthanide cation and 2 mM 4-ICA at variable pH. Dashed curves show the species distribution in mole % of the metal given on the right axis. The solid line in (E) is the theoretical profile calculated with eq 8 and rate constants given in text.

at variable pH. The last point from this series obtained with 5 mM Nd(III) is actually closer to the line for the 1:1 mixture.

The results of experiments with variable metal and ligand concentrations confirm the first-order kinetics in the respect of $\text{Nd}_2\text{L}(\text{OH})_5$ complex, but they also clearly show the existence of an inhibitory effect of the ligand. Figure 11 (solid squares) shows the effect of 4-ICA concentration on the reaction rate at fixed Nd(III) concentration and fixed pH

9. The strong observed inhibitory effect (k_{obs} decreases 30 times on going from 1 mM to 6 mM 4-ICA) is principally due to the shift in the species distribution (the fraction of $\text{Nd}_2\text{L}(\text{OH})_5$ complex decreases from 93% to 11%), but there is also an additional approximately 3-fold inhibitory effect. The open squares show the second-order rate constants calculated as the ratio $k_{\text{obs}}/[\text{Nd}_2\text{L}(\text{OH})_5]$, which tend to “saturate” at increased 4-ICA concentrations at a level

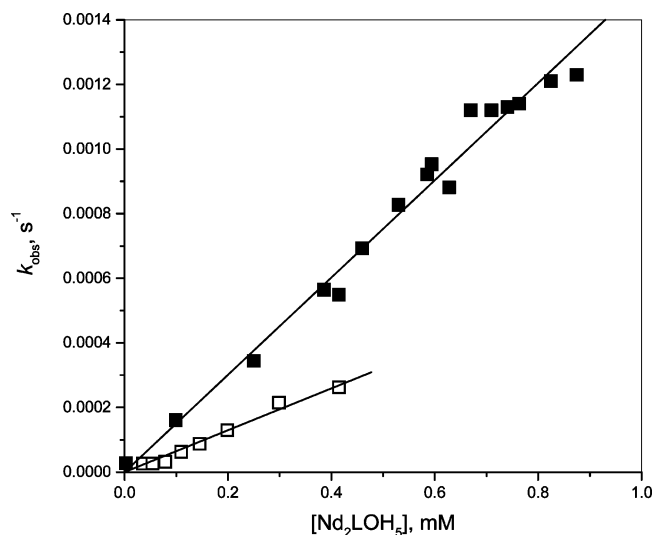


Figure 9. Observed first-order rate constants for the hydrolysis of BNPP by 2 mM Nd(III) in the presence of 2 mM (solid squares) and 4 mM (open squares) 4-ICA at variable pH plotted vs the calculated concentration of $\text{Nd}_2\text{L}(\text{OH})_5$ species.

approximately three times lower than the maximum value observed at small ligand concentrations. We were unable to quantify this inhibitory effect. Evidently the anion of 4-ICA interacts with the active species probably affording a complex of composition $\text{Nd}_2\text{L}_2(\text{OH})_5$ with a smaller catalytic activity, but titration data did not indicate the existence of such a complex. In principle, it can be overlooked in titration experiments because formation of this complex is significant only for large ligand concentrations, when the fraction of the pentahydroxo complex $\text{Nd}_2\text{L}(\text{OH})_5$ is small. Interestingly, other anions also inhibit the catalytic activity, some of them being even stronger inhibitors than 4-ICA, as will be discussed later.

With other lanthanides an approximately 3-fold similar inhibitory effect was observed under an excess of 4-ICA.

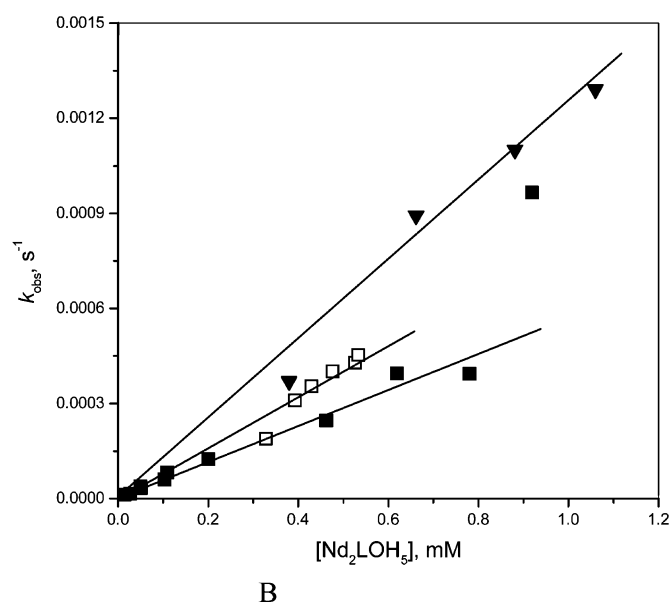
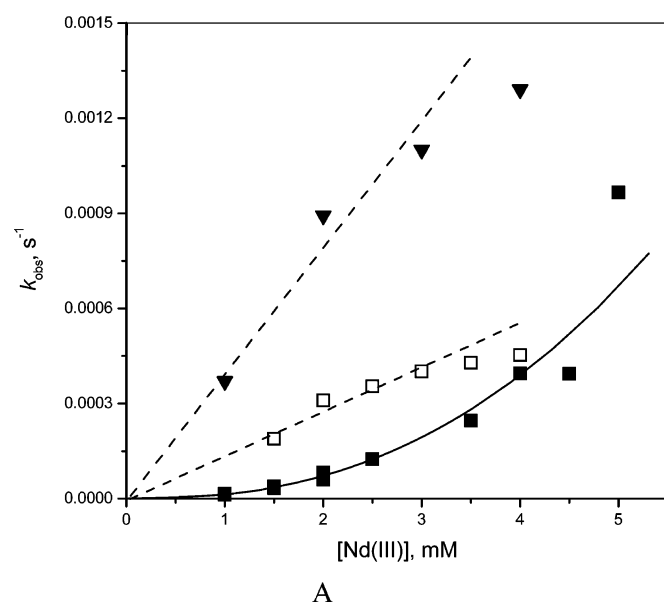


Figure 10. (A) Dependences of observed first-order rate constants for the hydrolysis of BNPP by Nd(III) on metal ion concentration: solid triangles, results obtained at $[\text{Nd(III)}]:[4\text{-ICA}] = 1:1$; open squares, results obtained at $[\text{Nd(III)}]:[4\text{-ICA}] = 1:1.5$; solid squares, results obtained at fixed $[4\text{-ICA}] = 6$ mM. (B) Same results replotted as dependences of k_{obs} on calculated concentration of $\text{Nd}_2\text{L}(\text{OH})_5$ species in each series.

Formal extrapolation of the second-order rate constants obtained under different conditions with the more extensively studied Nd(III) to zero ligand concentration showed that results obtained with 1:1 metal-to-ligand ratio give a rate constant which is just 20% lower than the extrapolated one for the zero ligand concentration. Therefore, we consider the second-order rate constants obtained under these conditions as reasonably close estimates of the true rate constants for the respective active species. Figure 12 shows all k_{obs} values obtained at M:L ratio 1:1 for all lanthanides studied (results for Dy(III) are corrected for the contribution of $\text{Dy}(\text{OH})_2^{2+}$ as described below) plotted vs calculated concentrations of the active species: $\text{M}_2\text{L}_2(\text{OH})_4$ for La(III) and Pr(III) and $\text{M}_2\text{L}(\text{OH})_5$ for Eu(III) and Dy(III). The slopes of these plots and the slope of the respective plot for Nd(III) (Figure 9, solid squares) are regarded as the second-order rate constants for the cleavage of BNPP by the respective hydroxo complexes in accordance with eqs 6 and 7.

$$k_{\text{obs}} = k_{24}[\text{M}_2\text{L}_2(\text{OH})_4] \quad \text{M} = \text{La, Pr} \quad (6)$$

$$k_{\text{obs}} = k_{25}[\text{M}_2\text{L}(\text{OH})_5] \quad \text{M} = \text{Nd, Eu} \quad (7)$$

The situation with Dy(III) was more complex. Results in Figure 8E clearly show that for this cation lower hydroxo complexes also contribute to the observed reactivity. To identify contributions of individual species, k_{obs} was considered to be a linear combination of contributions from all hydroxo complexes observed for Dy(III), eq 8.

$$k_{\text{obs}} = k_{11}[\text{M}(\text{OH})_2^{2+}] + k_{23}[\text{M}_2\text{L}_3(\text{OH})_3] + k_{24}[\text{M}_2\text{L}_2(\text{OH})_4] + k_{25}[\text{M}_2\text{L}(\text{OH})_5] \quad (8)$$

The multiparameter fitting of all results obtained for this cation to eq 8 showed that only two contributions are significant: from $\text{M}(\text{OH})_2^{2+}$ and $\text{M}_2\text{L}(\text{OH})_5$ species. The solid line in Figure 8E is drawn in accordance with the eq 8 with

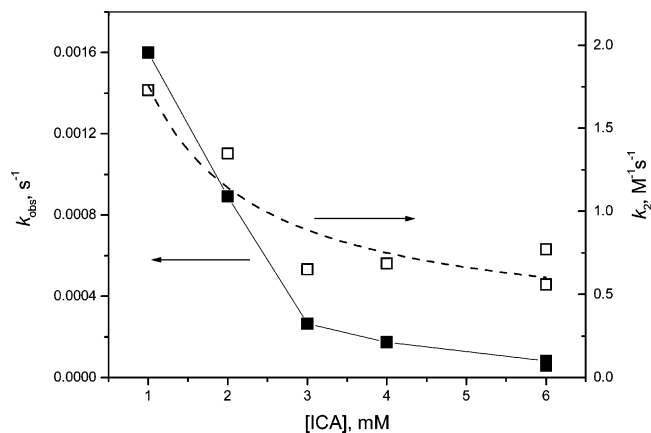


Figure 11. Observed first-order rate constants for the hydrolysis of BNPP by 2 mM Nd(III) in the presence of variable concentration of 4-ICA (solid squares). Open squares (right axis) show the values of second-order rate constants calculated as the ratio $k_{\text{obs}}/[\text{Nd}_2\text{L}(\text{OH})_5]$ at each 4-ICA concentration. Lines are not the fitting curves; they are drawn to better visualize the tendencies.

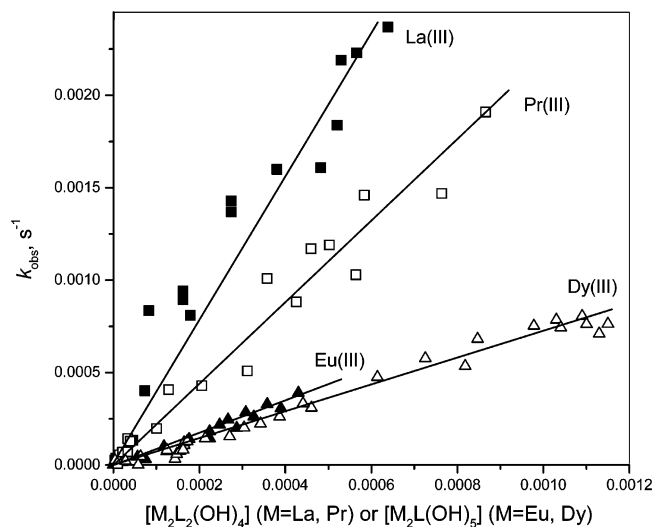


Figure 12. Dependences of observed first-order rate constants for the hydrolysis of BNPP by different lanthanide cations obtained at $[\text{M}]:[\text{4-ICA}] = 1:1$ on concentrations of $\text{M}_2\text{L}_2(\text{OH})_4$ species for $\text{M} = \text{La(III)}$ and Pr(III) or $\text{M}_2\text{L}(\text{OH})_5$ species for $\text{M} = \text{Eu(III)}$ and Dy(III) . In the case of Dy(III) , the rate constants are corrected for the contribution of $\text{Dy}(\text{OH})^{2+}$ species (see text).

$k_{11} = 0.83 \text{ M}^{-1} \text{ s}^{-1}$, $k_{23} = k_{24} = 0$, and $k_{25} = 0.69 \text{ M}^{-1} \text{ s}^{-1}$. Figure 12 (open triangles) shows k_{obs} for Dy(III) corrected for the contribution of DyOH^{2+} as $(k_{\text{obs}} - 0.83[\text{DyOH}^{2+}])$ plotted vs $[\text{Dy}_2\text{L}(\text{OH})_5]$. The slope of this line gives the k_{25} value coinciding with that found from the fitting of the pH profile in Figure 8E. The second-order catalytic rate constants k_{c} , which equal either k_{24} (for La(III) and Pr(III)) or k_{25} (for Nd(III) , Eu(III) , and Dy(III)), for the cleavage of BNPP by hydroxo complexes of all lanthanides studied are collected in Table 2.

Kinetics of the hydrolysis of two other phosphoester substrates HPNPP and DPNPP was studied in less details in the presence of La(III) , Nd(III) , and Dy(III) . Figure 13 shows the rate vs pH profiles and their fit (solid lines) to eq 8. In the case of La(III) , besides $\text{La}_2\text{L}_2(\text{OH})_4$ species there is also a contribution from the mononuclear $\text{LaL}(\text{OH})$ species, with rate constants $3.5 \pm 0.1 \text{ M}^{-1} \text{ s}^{-1}$ for HPNP and 0.4 ± 0.1

$\text{M}^{-1} \text{ s}^{-1}$ for DPNPP. The respective k_{24} values are given in Table 2. For Nd(III) only the pentahydroxo complex $\text{Nd}_2\text{L}(\text{OH})_5$ was reactive with both substrates, and for Dy(III) the $\text{Dy}(\text{OH})^{2+}$ species was as active as $\text{Dy}_2\text{L}(\text{OH})_5$ with $k_{11} = 11.8 \pm 0.8 \text{ M}^{-1} \text{ s}^{-1}$ for HPNP and $0.54 \pm 0.23 \text{ M}^{-1} \text{ s}^{-1}$ for DPNPP (for k_{25} values, see Table 2).

A qualitative inspection of the results collected in Table 2 reveals a strong shift in the relative reactivity of phosphate esters of different types in catalytic as compared to alkaline hydrolysis. The most reactive toward free hydroxide NPDPP becomes the least reactive substrate toward metal hydroxo complexes. Also HPNPP, which is 10^4 times more reactive than BNPP toward free hydroxide, is only 3 to 10 times more reactive than BNPP in the catalytic reaction. Table 2 also provides the ratios of catalytic second-order rate constants for active hydroxo species (k_{c}) to the rate constants of the alkaline hydrolysis (k_{OH}) of the same substrates. By this parameter the lanthanide complexes are superior to free hydroxide by a factor of 10^5 toward BNPP and 10^2 toward HPNPP and have the same reactivity as free OH^- toward DPNPP. In terms of often cited ‘‘catalytic effect’’ defined as the ratio of the observed rate constants in the presence and in the absence of catalyst under similar conditions, lanthanide hydroxo complexes stabilized by 4-ICA are among the most active. Thus, in the presence of 2 mM La(III) and 2 mM 4-ICA at pH 9 k_{obs} is enhanced by a factor of 10^7 for BNPP, by 3×10^4 for HPNPP, and by 10^2 for DPNPP.

A common feature for all substrates employed is that the highest reactivity is always observed for a complex with largest number of bound hydroxo ligands. Similar trends in BNPP hydrolysis were reported also for binuclear Zn(II) complexes of general type $\text{LZn}_2(\text{OH})_n^{4-n}$, where L is an organic ligand and n ranges from 1 to 3,^{37,38} as well as for pyrazolate-based dizinc(II) complexes.³⁹ It was interpreted as follows: the first hydroxide always serves as a bridging ligand and loses its nucleophilic reactivity because it is too tightly bound to both metal ions, while either the second or the third hydroxides may be terminal and more reactive or may weaken the binding of the bridging hydroxide. Similarly in our system all hydroxides in the trihydroxo complex may be bridging and nonreactive, but tetra- and pentahydroxo complexes should have at least some terminal hydroxides (see the above discussion of possible complexes structures). Low reactivity of bridging hydroxides is confirmed also by results reported for extensively studied Co(III) binuclear hydroxo complexes, which involve the fragment $\text{Co}(\mu_2\text{-OH})_2\text{-Co}$: bridging hydroxides do not have any nucleophilic reactivity until one of them becomes deprotonated affording $\mu_2\text{-O}^{2-}$ anion acting as a nucleophile.⁴⁰

On the other hand the reactivity of binuclear La(III) methoxo complexes $\text{La}_2(\text{OME})_n^{6-n}$ in methanolysis of both

(37) Arca, M.; Bencini, A.; Berni, E.; Caltagirone, C.; Devillanova, F. A.; Isaia, F.; Garau, A.; Giorgi, C.; Lippolis, V.; Perra, A.; Tei, L.; Valtancoli, B. *Inorg. Chem.* **2003**, *42*, 6929.

(38) (a) Bencini, A.; Berni, E.; Bianchi, A.; Fedi, V.; Giorgi, C.; Paoletti, P.; Valtancoli, B. *Inorg. Chem.* **1999**, *38*, 6323. (b) Bazzicalupi, C.; Bencini, A.; Bianchi, A.; Fusi, V.; Giorgi, C.; Paoletti, P.; Valtancoli, B.; Zanchi, D. *Inorg. Chem.* **1997**, *36*, 2784.

(39) Bauer-Siebenlist, B.; Meyer, F.; Farkas, E.; Vidovic, D.; Cuesta-Seijo, J. A.; Herbst-Irmer, R.; Pritzkow, H. *Inorg. Chem.* **2004**, *43*, 4189.

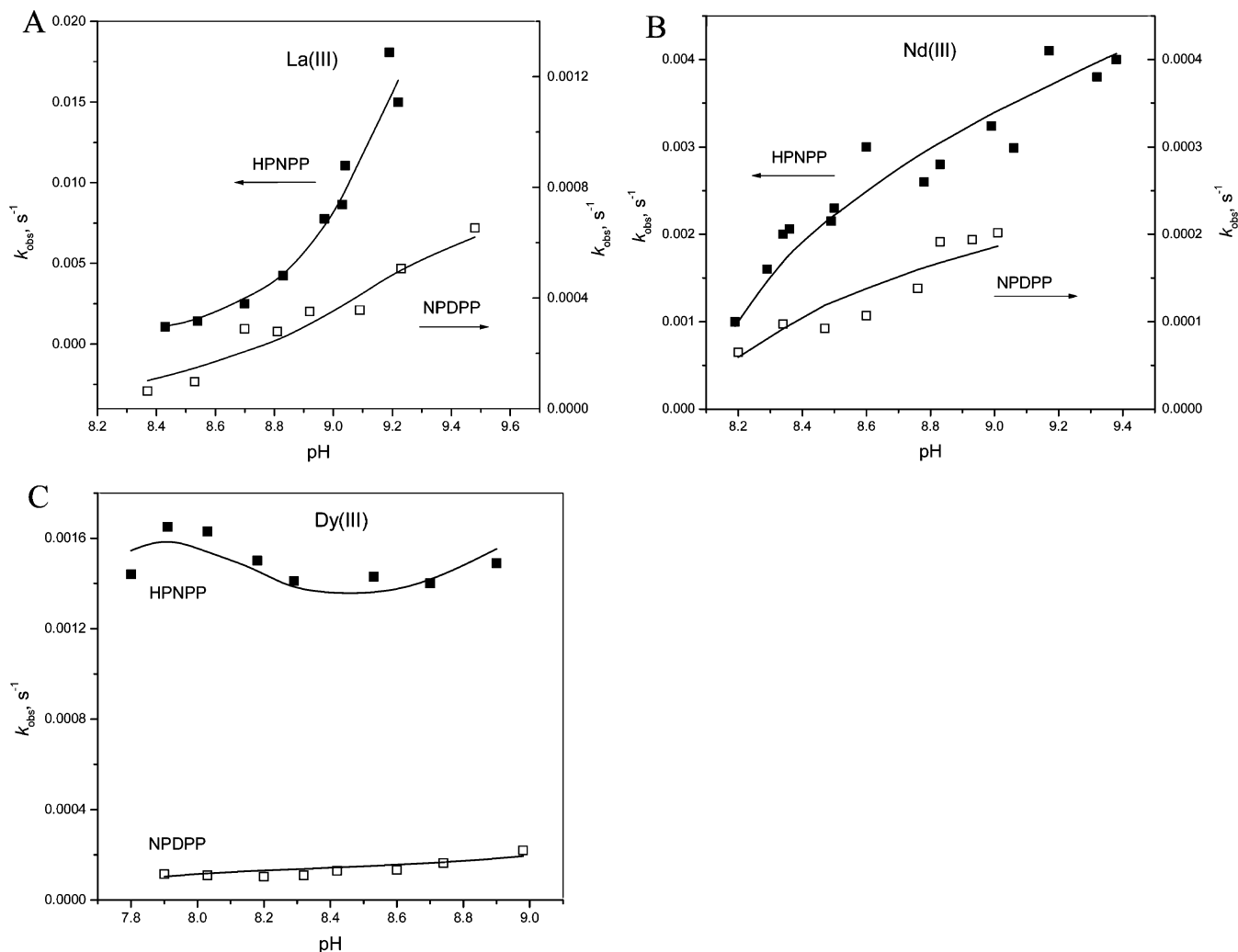


Figure 13. Observed first-order rate constants for the hydrolysis of HPNPP (solid squares) and NPDPP (open squares) by different metals in the presence of 2 mM lanthanide cation and 2 mM 4-ICA at variable pH. Solid lines are the theoretical profiles calculated using eq 8 with rate constants for individual hydroxo complexes given in Table 2 (for $M_2L_2(OH)_4$ and $M_2L(OH)_5$ species) and in the text (for other species): A, La(III); B, Nd(III); C, Dy(III).

Table 2. Second-Order ($M^{-1} s^{-1}$) Catalytic Rate Constants k_C (k_{24} or k_{25} Depending on the Type of Active Species) for the Cleavage of Phosphate Esters by Hydroxo Complexes of Lanthanides Stabilized by 4-ICA and by Free Hydroxide (k_{OH}) at 25 °C

active species	BNPP		HPNPP		NPDPP	
	k_C or k_{OH}	k_C/k_{OH}	k_C or k_{OH}	k_C/k_{OH}	k_C or k_{OH}	k_C/k_{OH}
OH^-	$(1.08 \pm 0.02) \times 10^{-5}$		0.12 ± 0.01		0.42 ± 0.07	
$La_2L_2(OH)_4$	4.0 ± 0.2	3.7×10^5	41 ± 4	330	0.76 ± 0.09	1.8
$Pr_2L_2(OH)_4$	2.19 ± 0.08	2.0×10^5				
$Nd_2L(OH)_5$	1.49 ± 0.06	1.4×10^5	4.9 ± 0.2	39	0.27 ± 0.01	0.64
$Eu_2L(OH)_5$	0.84 ± 0.02	7.8×10^4				
$Dy_2L(OH)_5$	0.69 ± 0.02	6.4×10^4	3.7 ± 0.2	30	0.45 ± 0.06	1.1

carboxylate esters and phosphate triesters increases on increase in n from 1 to 3 but then decreases for higher complexes with $n = 4$ and 5.⁴¹ The mechanism proposed for the reaction proceeding via the $La_2(OMe)_2^{4+}$ complex involves an opening of one of the bridges in the catalyst–substrate complex and subsequent nucleophilic attack of the terminal methoxide on the adjacent metal-bound substrate. The reason for decreased reactivity of complexes with larger

values of n was not discussed, but in fact the existence of an optimum number of bound methoxide (or hydroxide in aqueous systems) anions is not surprising taking into account two opposite trends associated with increase in their number: favorable enhancement of nucleophilic reactivity of bound anions and unfavorable decrease of the total positive charge of the complex. In our case the reactive species are neutral complexes which indeed may have a very low affinity to the substrate. A simple way to test the ability of catalytically active species to bind substrates is to measure the inhibitory effect by a nonreactive substrate analogue.⁴² Addition of diphenyl phosphate as a substrate analogue as well as of monophenyl phosphate (considered as a transition

(40) (a) Williams, N. H.; Cheung, W.; Chin, J. *J. Am. Chem. Soc.* **1998**, *120*, 8079. (b) Humphry, T.; Forconi, M.; Williams, N. H.; Hengge, A. C. *J. Am. Chem. Soc.* **2002**, *124*, 14860.

(41) (a) Neverov, A. A.; Gibson, G.; Brown, R. S. *Inorg. Chem.* **2003**, *42*, 228. (b) Tsang, J. S.; Neverov, A. A.; Brown, R. S. *J. Am. Chem. Soc.* **2003**, *125*, 7602.

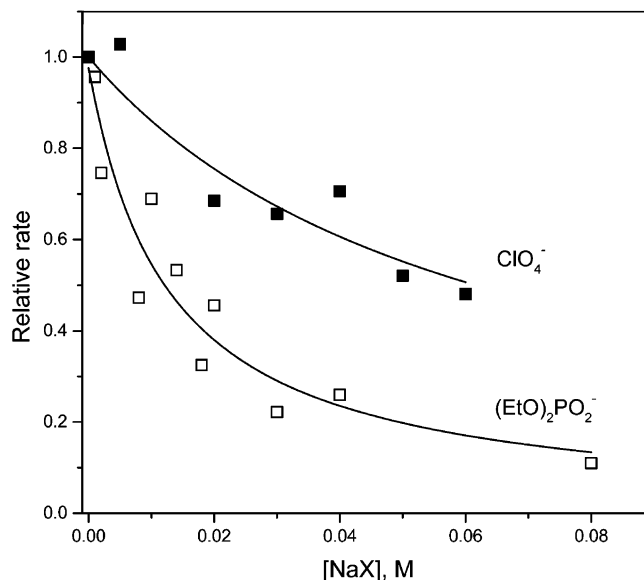
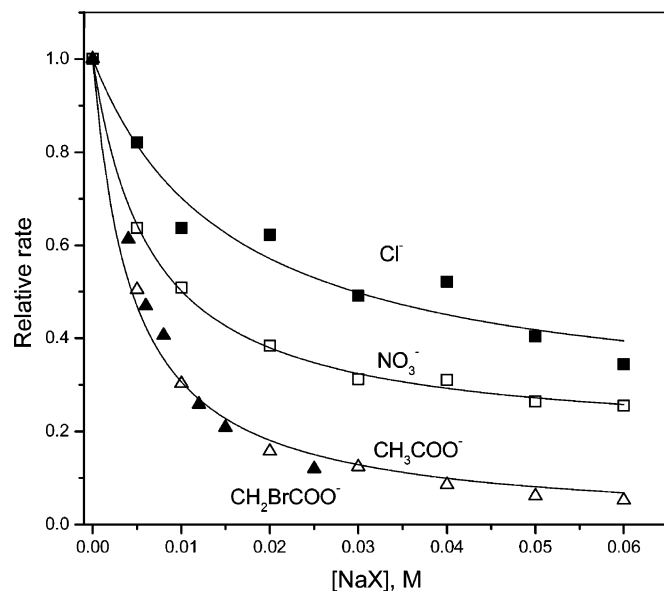


Figure 14. Inhibitory effects of anions (X) on the BNPP hydrolysis by 2 mM Nd(III) in the presence of 2 mM 4-ICA at pH 8.5.

Table 3. Apparent Binding Constants ($K_{X,app}$) of Anions to the Catalytically Active Form of Nd(III) Calculated by Fitting the Results in Figure 14 to Eq 12 and Stability Constants (K_1) of 1:1 Complexes of These Anions with Nd^{3+} Aquo Ion

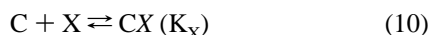
anion	$K_{X,app}$ ($\pm 10\%$), M^{-1}	K_1 , M^{-1} ^a
ClO_4^-	16	0.6
Cl^-	65	0.8
NO_3^-	150	2.0
$(EtO)_2PO_2^-$	80	100 ^b
CH_3COO^-	230	130 ^c
CH_2BrCOO^-	200	20 ^c

^a Stability constants taken from ref 19 at 25 °C and ionic strength 1.0.

^b From ref 43 at zero ionic strength. ^c At ionic strength 0.1.

state analogue)¹⁴ induced precipitation. The measurements were possible with diethyl phosphate, and in the course of this study, we found that many simple monoanions caused unexpectedly strong inhibitory effects.

Figure 14 shows the relative first-order rate constants for the hydrolysis of BNPP by Nd(III) in the presence of 4-ICA at fixed pH 8.4 as a function of added sodium salts of different anions. All these plots fit satisfactorily to eq 12 derived for a simplified scheme (9)–(11).



$$k_{obs}/k_{obs}^0 = (1 + (k_X/k_C)K_X[X]) / (1 + K_X[X]) \quad (12)$$

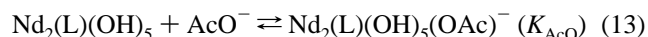
In these equations C is the catalytic species, S is the substrate, P is the reaction product(s), and X is the added anion. Table 3 lists the apparent binding constants for all anions employed obtained by the least-squares fitting of the results in Figure 14 to eq 12. For comparison Table 3 provides also the

(42) Iranzo, O.; Kovalevsky, A. Y.; Morrow, J. R.; Richard, J. P. *J. Am. Chem. Soc.* **2003**, *125*, 1988.

(43) Siniavskaja, E. I.; Sheka, Z. A. *Radiokhimiya* **1966**, *8*, 410.

stability constants (K_1) of 1:1 complexes of these anions with Nd^{3+} aquo ion taken from the literature. Values of $K_{X,app}$ for nitrate anion were determined also for other lanthanides, but no clear trend was observed ($K_{NO_3,app} = 65, 33, 82,$ and $30 M^{-1}$ for La, Pr, Eu, and Dy, respectively).

Complex formation between Nd(III) and acetate was studied also independently by spectrophotometric and potentiometric titrations. Additions of NaOAc to the solution containing an equimolar mixture of Nd(III) and 4-ICA adjusted to pH 8.4 produced small but clearly detectable changes in the hypersensitive region from which one may estimate the apparent binding constant $K_{OAc,app} = 220 \pm 40 M^{-1}$ (see Figures 4S and 5S in Supporting Information) close to that found from kinetic experiments. Figure 15A shows potentiometric titration curves for the mixture of Nd(III) and 4-ICA in the absence and in the presence of added NaOAc. The curves coincide until consumption of 1 equiv of the base, but after that the curve obtained in the presence of acetate is shifted downward indicating an increased stability of higher hydroxo complexes. Fitting of the titration curves obtained in the presence of increased amounts of acetate to the reaction scheme (1)–(4) gives stability constants for trihydroxo and tetrahydroxo complexes coinciding within the limits of experimental errors with those obtained in the absence of acetate but increased values for the stability constant for the pentahydroxo complex. This can be attributed to the formation of $Nd_2(L)(OH)_5(OAc)^-$ species in accordance with eq 13.



The expression for the observed β_{21-5} value will take the form

$$\beta_{21-5,obs} = \beta_{21-5}(1 + K_{AcO}[AcO^-]) \quad (14)$$

Figure 15B shows the plot of $\beta_{21-5,obs}/\beta_{21-5}$, the slope of which equals $K_{AcO} = 725 \pm 40 M^{-1}$. This value is

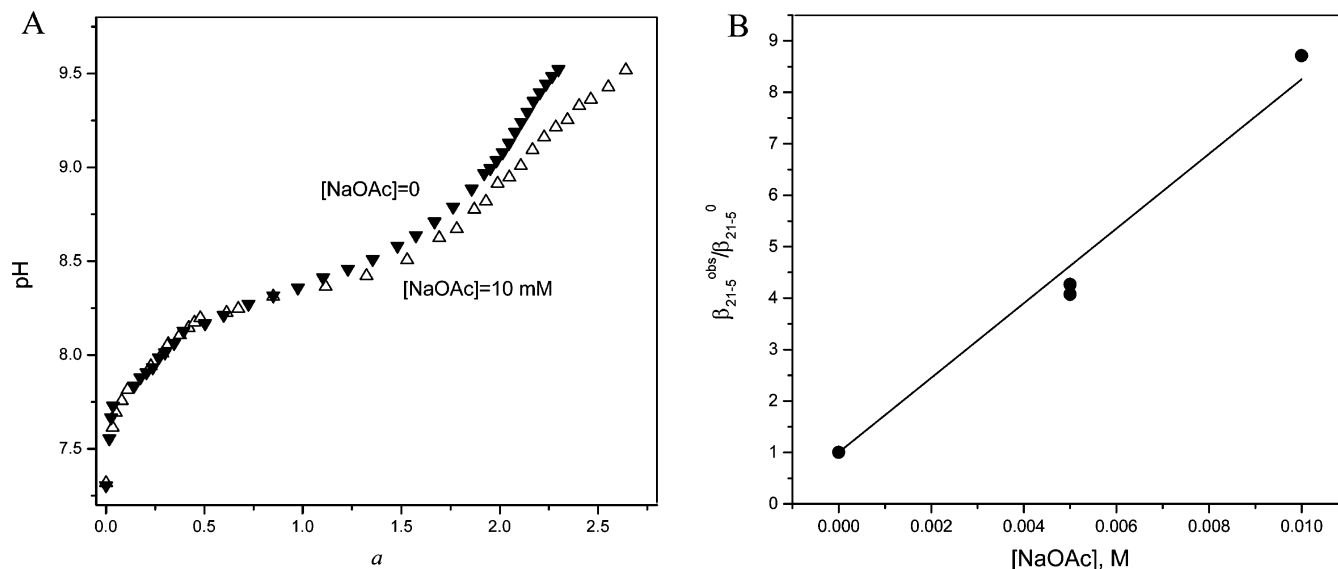


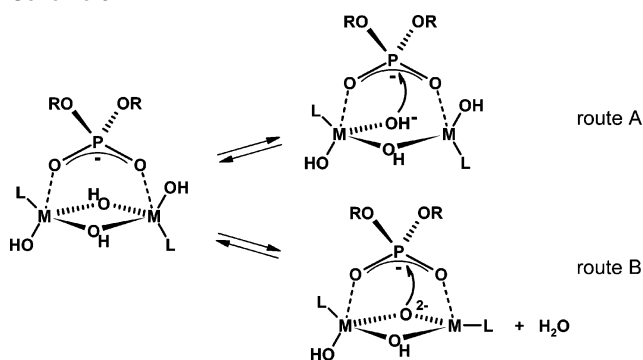
Figure 15. (A) Titration curves for the mixture of 2 mM ICA and 2 mM Nd(III) in the absence (solid triangles) and in the presence of 10 mM NaOAc (open triangles). (B) Relative apparent formation constant for the $\text{Nd}_2\text{L}(\text{OH})_5$ complex as a function of concentration of added sodium acetate.

significantly higher than that obtained from the inhibitory effect (Table 3) and by spectrophotometry, but it is necessary to take into account that kinetically and spectrophotometrically determined apparent binding constants were obtained under conditions when only 40% of Nd(III) is present in the form of $\text{Nd}_2(\text{L})(\text{OH})_5$ and therefore $K_{X,app}$ should be less than its true value by a factor of 2.5 in agreement with observed results.

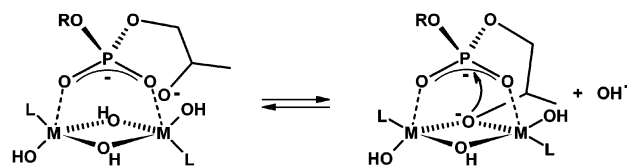
As is evident from results in Table 3, the neutral hydroxo complex not only binds the substrate analogue diethyl phosphate with the same strength as highly charged aquo cation Nd^{3+} but surprisingly shows unusually high affinity to other simple anions such as chloride or nitrate, which practically do not interact with Nd^{3+} . Obviously the above-mentioned inhibitory effect of the excess of 4-ICA has the same origin. There is no correlation between binding constants of anions and their basicity. The largest binding constants are observed for planar anions which probably fit better to the catalyst binding site. We suppose that these anions bind to the binuclear active species by the same mode as that reported for amino acid zwitterions in tetranuclear hydroxo complexes (Chart 1c) and that the binuclearity of these species is a reason for their increased affinity to anions.

In view of these considerations the most plausible mode of catalyst–substrate interaction is a bridging coordination of a phosphodiester anion to the binuclear catalytic species sketched in Scheme 3. In this case the best positioned for the nucleophilic attack hydroxide is one of the bridging anions and a possible role of additional hydroxides is to facilitate an opening of the bridge (route A). On the other hand it seems possible that an additional hydroxide may reversibly deprotonate the bridging hydroxide with elimination of a water molecule and creation of a much more nucleophilic oxo bridge (route B) which serves as a nucleophile in binuclear Co(III) complexes⁴⁰ (see above). Several oxo-bridged polynuclear lanthanide complexes were described in the literature usually with a μ_4 - or μ_6 -OXO

Scheme 3



Proposed mechanism for BNPP hydrolysis



Proposed mechanism for HPNPP hydrolysis

ligand.^{10a,11} Binuclear peroxo complexes with a doubly deprotonated O_2^{2-} bridge are readily formed in weakly basic lanthanide solutions of hydrogen peroxide and possess a very large phosphodiesterolytic activity.^{44,45} Of course, hydrogen peroxide is a more acid molecule than water, but formation of even a small fraction of highly reactive oxo anions may be sufficient for the observed reactivity.

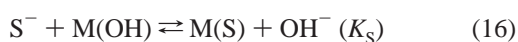
The outlined above mechanism may operate for both BNPP and NPDPP substrates with an obvious difference of a very low affinity of the triester substrate to the catalyst. The gradual decrease of activity of lanthanides in BNPP

(44) Takasaki, B. K.; Chin, J. *J. Am. Chem. Soc.* **1995**, *117*, 8582.

(45) Mejía-Radillo, Y.; Yatsimirsky, A. K. *Inorg. Chim. Acta* **2003**, *351*, 97.

hydrolysis on going from La(III) to Dy(III) does not have a simple explanation. For lanthanide aquo ions the activity trend is opposite and reflects expected stronger electrophilic substrate activation by heavier more acid cations.⁴⁶ However, this trend is partly attributable to decreased pK_a values of heavier lanthanides and therefore the higher fraction of their hydroxo complexes presenting in the solution at pH about 7 employed in studies with aquo ions. The reactivity of hydroxide complexes of different lanthanides stabilized by Bis-Tris propane follows the same trend as in the case of 4-ICA complexes.¹⁸ Also with methoxide lanthanide complexes the highest reactivity is observed for La(III).⁴⁷ An obvious problem in interpretation of these trends is that composition of reactive species may vary for different lanthanides, as is the case for 4-ICA complexes. A stronger deactivation of the bound nucleophile is a possible though only qualitative explanation of the lower activity of heavier cations. Of course, one cannot exclude a kinetically equivalent mechanism with external hydroxide as a nucleophile and a lanthanide complex with one less hydroxide as an active species, which would have a lower concentration for smaller cations.

The situation with HPNPP should be different since the hydrolysis of this substrate proceeds via a different mechanism, Scheme 1. The efficiency of catalysis with HPNPP is lower than with BNPP in this case; although similar and higher than in water, the efficiency of La(III) in methanolysis of both substrates was reported in anhydrous methanol.^{32,48} The different efficiency of catalysis may be related to different roles played by the metal-bound hydroxide in the cleavage of these substrates. For BNPP it acts as a nucleophile, but hydrolysis of HPNPP proceeds via preliminary equilibrium deprotonation of the 2-hydroxy group, which does not need any participation of the metal-bound hydroxide (at equilibrium the degree of deprotonation depends only on pH and pK_a of the hydroxyl group). Nevertheless the analysis of rate vs pH profiles with this substrate agrees with the involvement of the same active hydroxo complexes as for BNPP for all lanthanides studied. A possible explanation of this is that the alkoxide group of the deprotonated HPNPP should be placed at the same position inside the catalyst–substrate complex as the hydroxide in the reaction with BNPP. This will require the substitution of one of the bridging hydroxides by the alkoxide group as illustrated in Scheme 3. In a very simplified form the kinetic scheme corresponding to such mechanism is given by eqs (15)–(17), where SH stays for HPNPP and M(OH) is the active hydroxo complex.



(46) Roigk, A.; Hettich, R.; Schneider, H.-J. *Inorg. Chem.* **1998**, *37*, 751.

(47) Lewis, R. E.; Neverov, A. A.; Brown, R. S. *Org. Biomol. Chem.* **2005**, *3*, 4082.

(48) Tsang, J. S. W.; Neverov, A. A.; Brown, R. S. *J. Am. Chem. Soc.* **2003**, *125*, 1559.

The expression for the observed first-order rate constant which follows from the scheme (15)–(17) takes the form of eq 18.

$$k_{\text{obs}} = k_{\text{MS}} K_{\text{OH}} K_{\text{S}} [\text{M(OH)}] \quad (18)$$

Evidently this expression coincides with the experimentally obtained rate law.

In terms of mechanisms outlined in Scheme 3, the lower efficiency of catalysis for HPNPP as compared to BNPP can be explained as follows. In the case of BNPP the catalyst provides the electrophilic assistance to the nucleophilic attack on the phosphoryl group and transforms the hydroxide from an intermolecular to an intramolecular nucleophile. The latter effect can be very significant in view of often observed very large “effective molarities” for nucleophilic reactions.⁴⁹ In the case of HPNPP this effect is absent because the nucleophile is already intramolecular and the observed efficiency of catalysis is lower.

In conclusion, we point out that using low basic amino carboxylates derived from nitrogen heterocycles as stabilizing ligands for lanthanide hydroxo complexes seems to be a promising approach to more stable and active catalysts. Second-order rate constants observed with lanthanide complexes stabilized by 4-ICA for the cleavage of diester substrates are among the largest reported so far in the literature. Perhaps the most interesting is the observation of maximum activity for higher neutral hydroxo complexes which surprisingly display a high affinity to anionic species. Previously we observed a similar trend in activity for lanthanide hydroxo complexes stabilized by a neutral amino alcohol ligand,^{18,30} and interestingly, the absolute reactivities of hydroxo complexes stabilized by a neutral ligand were lower than those we observe now with an anionic stabilizing ligand. In line with this, we found recently that active forms of the Ce(IV) catalyst are also nearly neutral hydroxo/oxo species.⁵⁰ Therefore, it seems that the total charge of lanthanide hydroxo complexes is not of a primary importance. More important are the polynuclearity of the active species and a certain way of binding of the stabilizing ligand.

Acknowledgment. We thank the DGAPA-UNAM for financial support (Project IN 204805). F.A.-P. thanks CONACyT for a doctoral fellowship.

Supporting Information Available: A table containing values of logarithms of the overall formation constants and statistical fitting parameters of lanthanide complexes with 4-ICA from all titration experiments, pH profiles for Bjerrum functions \bar{n} and their detailed discussion, figures showing the absorbance of a mixture of Nd(III) and 4-ICA at 578 nm as a function of pH superimposed with the species distribution diagram, absorption spectra of a mixture of Nd(III) and 4-ICA in the hypersensitive region at increased concentrations of NaOAc, and a Benesi–Hildebrand plot for the spectrophotometric titration of a mixture of Nd(III) and 4-ICA with sodium acetate.

IC061024V

(49) Kirby, A. J. *Adv. Phys. Org. Chem.* **1980**, *17*, 183.

(50) Maldonado, A. L.; Yatsimirsky, A. K. *Org. Biomol. Chem.* **2005**, *3*, 2859.